

# The swim-survey archive of the Mediterranean rocky coasts: Potentials and future perspectives

Stefano Furlani<sup>a,\*</sup>, Fabrizio Antonioli<sup>b</sup>

<sup>a</sup> *University of Trieste, Department of Mathematics and Geosciences, Trieste, Italy*

<sup>b</sup> *CNR, IGAG, Rome, Italy*

---

## A B S T R A C T

The Geoswim programme is an expedition-type project which is aiming to survey, monitor and measure the entire perimeter of rocky coasts of the Mediterranean Sea. The project officially started in 2012 with the first one-man survey of 193.4 km by snorkeling along the northeastern Adriatic coasts, and is ongoing. So far, 559.5 km of rocky coasts have been surveyed, over 98 days of survey, and several hundred thousand time-lapse images, continuous videos and outline images have been collected, both above and below the waterline. Bathymetric data and physical/chemical parameters, such as temperature and electrical conductivity have also been collected during the snorkel surveys. Instruments are hosted on a specially-built raft, called instrumental-supported raft (ISR). The data are not homogeneous because over the years the approach has changed following the introduction of new technologies and some redesign of the instruments used, and, in part, also the type of data collected. Moreover, observational data for use in coastal studies and for integrating instrumental data are collected. The paper presents and take stock of the geometry of the database and discusses the main results of the Geoswim programme.

Data analysed highlighted that the database is a significant archive that provides 1) images and videos as a baseline for subsequent comparisons, 2) large amount of images to be used to build 3D models of coastal landforms, 3) data for statistics, and 4) a valuable source of possible discoveries of unknown coastal objects, such as sea caves, tidal notches at unexpected sites, ecological observations, etc.

---

## 1. Introduction

Rocky coasts are erosional landforms which develop through the interplay of marine and subaerial processes acting at sea level (Kennedy et al., 2014). Although these coasts are erosional, the rate of shoreline retreat is slow due to the resistance of the bedrock to erosion. The type of rock and its lithification strongly influence the rate of erosion and consequently of the resulting landform. Typically, these coasts are dominated by exposed bedrock with steep slopes and high elevations adjacent to the shore. They exhibit high relief and rugged topography. Most studies on these coasts are carried out in selected sites, with point observations, while only short sectors are studied using wide field surveying approaches from the sea, mainly because of the difficult logistics (Furlani, 2020, and references therein). The Geoswim programme (<https://geoswim-eu.webnode.it/>) consists of snorkel surveys along long sectors of rocky coast in the Mediterranean Sea, which is particularly suitable for swimming given its favourable wave and tide

conditions (Furlani et al., 2014a; Morucci et al., 2016). Geoswim collects observational and instrumental data along daily routes up to 10-km long. Videos and time-lapse images are collected on a continual basis, while visual observations, such as coastal landforms, submarine springs, etc. are collected at prominent locations and are documented with outline images (Furlani et al., 2014b; Furlani et al., 2017a, 2017b, 2021b; Furlani, 2020).

Time-lapse images are used to build 3D models of the surveyed coast (Furlani et al., 2020). They are commonly used in geomorphology for building 3D models above or below the waterline (e.g. Barker et al., 1997; Chandler, 1999; Fraser and Cronk, 2009; Abadie et al., 2018; Fawcett et al., 2019), including through low-cost approaches (Gaglianone et al., 2018). The massive use of a photogrammetric approach and related methods, such as Structure from Motion (SfM), has greatly increased the need and use of images in the last decade (Micheletti et al., 2014). A wide use of this approach has also been carried out in rocky coastal environments, such as to study coastal landslides (e.g. Bennett

---

\* Corresponding author.

E-mail address: [sfurlani@units.it](mailto:sfurlani@units.it) (S. Furlani).

**Table 1**

Description of the instruments used during the 20 Geoswim campaigns. A) type of instrument, B) type of data acquired; C) model of the instrument; D) main technical features of the instrument; E) campaigns in which the tool was used with reference to [Table 2](#).

A Instrument	B Type of data acquired	C Model	D Features	E Expeditions
ISR	Hosting instruments	ISR1	Sporasub platform EVA, 1.15 m long, 0.57 m large	1, 3-4, 6-12, 14-
	Hosting instruments	ISR2	ISR home-made with two PVC waterproof tubes	2, 5
	Hosting instruments	ISR3	ISR with Polystyrene (EPS)	13
GPS	Latitude, longitude	Garmin e-trex 10	Precision = 10 m, freq = 1 s;	1-20
		GPS within cameras	Precision = 10 m, freq = 1 s;	14-20
Camera	Time-lapse images	GoPRO Hero	5 Mp, Freq = 1 image/s	1-9
	Time-lapse images	GoPRO Hero 6	12 Mp, Freq = 1 image/0.5 s	14-20
	Time-lapse images	Floureon Y8	14 Mp, Freq = 1 image/s	10
	Video 360	Insta 360	5.7 K	18
	Video 360	Insta 2360	5.7 K	20
	Video	Canon G12	720p	1-5
CTD sensor	Video	Floureon Y8	1080p	6
	T, EC	Eijkelpamp Soil & Water	IP68, EC = 0-120mS/cm; T sensor	1-20
Echosounder	T, EC	Geoswim sensor	EC = 0-120mS/cm; 5 T sensors	18
	Depth	Digital Sonar H22PX	depth: 0.8 to 61 m; water temp = 0.1 °C	1-11
lidar	Depth	Velixar T-Box Sonar Phone Sp200	depth: 0.6 to 73 m; water temp = 0.1 °C	14, 16
	Depth	Garmin Echomap 72 cv	Receiver GPS 5 Hz with CHIRP DownVu™	20
lidar	3D models	Iphone 12 Pro Max	Distance from 0.2 to 5 m	20
Cameras for outline images	Videos/images	GoPRO Hero 3	Video 4 K, 12 Mp, F2/8 ultra-wide angle	4-8
	Images	Canon PowerShot G12	Video HD 720, 10 MP	1-10
	Images	Nikon D700	Reflex 12 Mp	4-10
	Images	Panasonic Lumix S DC-5	DSLM, CMOS 25 Mp	
Drones	Images	Panasonic Lumix DC-G9	21 Mp	
	Videos/images	DJI Mavic 2 Pro	Video 4 K, 1" CMOS sensor, 20 Mp photographs, f/2.8-f/11	18, 21
	Videos/images	Autel nano plus	Video 4 K, 1/1.28 CMOS sensor, 50 Mp photographs, f/1.9	21
	Videos	DJI Mavic Mini	Video 2.7 K, 1/2.3" CMOS sensor, 12 Mp, f/2.8	18

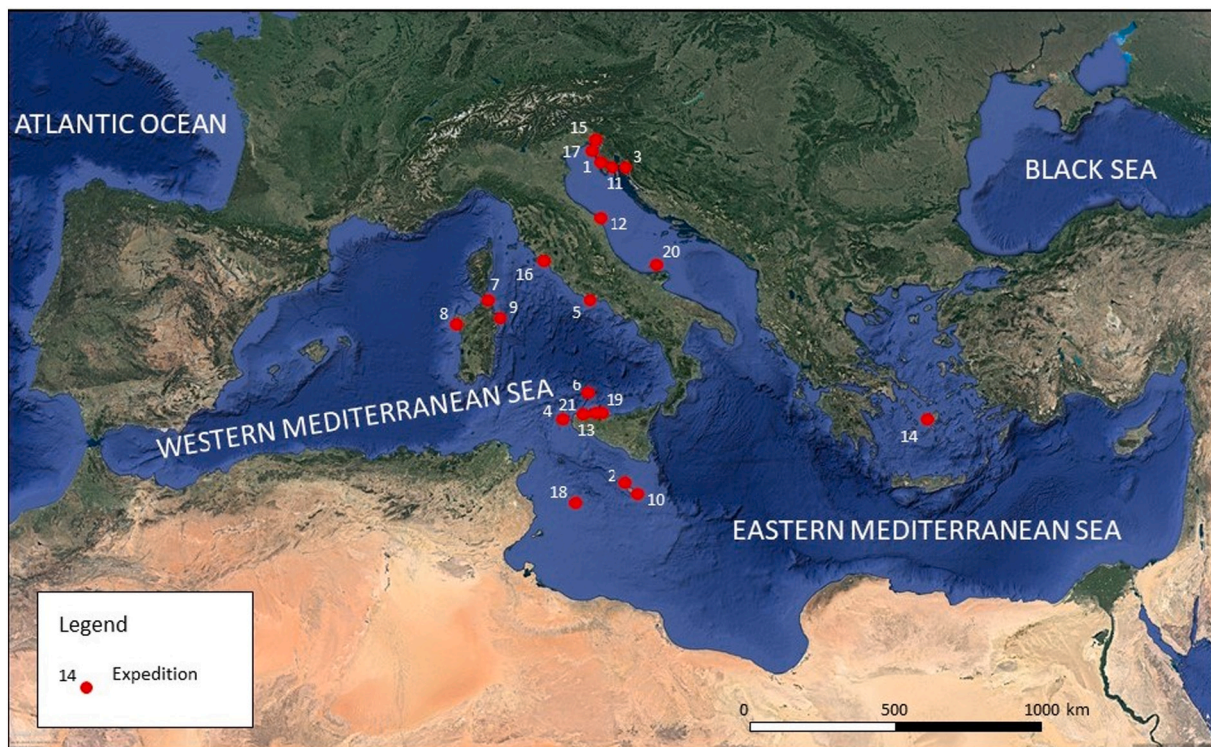


**Fig. 1.** The Mediterranean areas surveyed using the Geoswim approach so far. The numbers refer to the campaigns described in [Table 2](#).

**Table 2**

The 20 expeditions carried out since 2012 within the Geoswim programme (modified from [Furlani et al., 2021b](#)). A) ID number; B) year of survey; C) area of survey; D) videos (Y/N, above, below or at the waterline); E) time-lapse images (Y/N, above, below or at the waterline); F) outline images (Y/N); G) total length of coastline surveyed; H) days of survey for each expedition; I) papers published from each expedition (the columns in the Additional Material Table).

A ID	B Year	C Location	D Videos (Y/N, a/b/w, duration (hours))	E Time-lapse images (Y/N, a/b/w)	F Outline images (Y/N, a/b)	G Total length (km)	H Days of survey	I Literature
1	2012	W Istrian Peninsula (Croatia, Slovenia, Italy)	(Y, a/b)	(N)	(Y, a/b)	253,2	27	<a href="#">Furlani, 2012</a> ; <a href="#">Furlani et al., 2014a</a>
2	2013	Gozo and Comino (Malta)	(Y, a/b)	(N)	(Y, a/b)	57	7	<a href="#">Furlani et al., 2017a</a>
3	2013	Stara Baska (Krak, Croatia)	(Y, a/b)	(N)	(Y, a/b)	2,2	1	/
4	2014	Egadi Islands (Italy)	(Y, w)	(N)	(Y, a/b)	67	7	<a href="#">Buseti et al., 2015</a> <a href="#">Furlani et al., 2021b</a> <a href="#">Antonioli et al. 2021</a>
5	2015	Gaeta Promontory (Latium, Italy)	(Y, w)	(N)	(Y, a/b)	2,5	1	<a href="#">Furlani et al., 2021b</a>
6	2015	Ustica (Sicily, Italy)	(N)	(N)	(Y, a/b)	14	2	<a href="#">Furlani et al., 2017b</a>
7	2015	Razzoli, Budelli, Santa Maria (Sardinia, Italy)	(N)	(Y, w)	(Y, a/b)	22,5	3	<a href="#">Furlani et al., 2021b</a>
8	2015	Capo Caccia (Sardinia, Italy)	(N)	(Y, w)	(Y, a/b)	26	2	<a href="#">Furlani et al., 2021b</a>
9	2015	Tavolara (Sardinia, Italy)	(N)	(Y, w)	(Y, a/b)	14,9	2	<a href="#">Furlani et al., 2021b</a>
10	2015	Malta (Malta)	(N)	(Y, w)	(Y, a/b)	19,2	3	<a href="#">Furlani et al., 2021b</a>
11	2015	SE Istria (Croatia)	(N)	(Y, w)	(N)	7	1	<a href="#">Vaccher, unpublished thesis</a>
12	2016	Monte Conero (W Adriatic Sea, Italy)	(N)	(Y, w)	(Y, a/b)	2,9	1	<a href="#">Furlani et al., 2018</a>
13	2016	Addaura (Palermo, Sicily, Italy)	(N)	(N)	(Y, a/b)	7	1	<a href="#">Caldareri et al., 2018</a>
14	2017	Paros (Greece)	(Y, w)	(Y, w)	(Y, a/b)	24	8	<a href="#">Furlani et al., 2021a</a>
15	2017	Sistiana-Duino (Gulf of Trieste, Italy)	(N)	(Y, a/b)	(N)	2	1	<a href="#">Furlani and Biolchi, 2018</a>
16	2018	Ansedonia and Argentario (Tuscany, Italy)	(Y, w)	(Y, a/b)	(Y, a/b)	10	2	<a href="#">Furlani et al., 2021b</a>
17	2019	Savudrija (Croatia)	(N)	(Y, a/b)	(N)	1.1	1	<a href="#">Furlani et al., 2021b</a>
18	2020	Isole Pelagie (Sicily, Italy)	(Y, a)	(Y, a/b)	(Y, a/b)	43.9	9	/
19	2020	Arenella (Sicily Italy)	(N)	(n, a/b)	(Y, a/b)	0.6	1	/
20	2021	Isole Tremiti (Puglia, Italy)	(Y, a/b)	(Y, a/b)	(Y, a)	5.7	1	/
TOTAL						535.3	81	

[et al., 2012](#); [Esposito et al., 2017](#); [Devoto et al., 2020, 2021](#)), shore platform processes (e.g. [Swirad et al., 2019](#)). Sonar data are commonly used to reconstruct the sea bottom near the coastline with a range of equipment being used to produce very detailed 3D models (e.g. [Levin et al., 2019](#)). Videos also support geomorphological studies both as field and laboratory support. Good results can be obtained with the use of “frame grabbed” video images, or time-lapse videos, to sequence geomorphic processes, such as in the study of beach movements ([Pitman, 2014](#)).

As far as temperature (T) and electrical conductivity (EC) are concerned, collected during the snorkeling at depths ranging from  $-0.15$  m to  $-0.50$  m, these can be used to identify freshwater outflows from submarine springs (e.g. [Furlani et al., 2014a, b, 2017a](#)). These are caused by the artesian flow of groundwater in response to pressure gradients in aquifers and breaches in confining layers ([Moore et al., 2009](#)). Several submarine springs were documented by [Furlani et al. \(2014b\)](#) in Istria (Croatia) and [Furlani et al. \(2017a\)](#) on the Gozo and Comino islands in the Maltese archipelago using lateral changes in the aforementioned parameters along the coastline. The evaluation of lateral variations of T and EC in the sea have been rarely used with bulk measurements ([Akawwi, 2008](#)), but usually in short, selected profiles ([Stieglitz et al., 2008](#)).

Other technologies have been used to map the underwater landscape using geophysical and photogrammetric sensors, such as USVs (Unmanned Surface Vessels), as described by [Mattei et al. \(2019\)](#). These type of approaches are optimized for underwater mapping ([Wynn et al., 2014](#); [Yoerger et al., 2007](#)).

In this paper, the set of instrumental and observational data collected by swimming and using an instrumental-supported raft (ISR), is here described. Moreover, the potentials and future perspectives of this type of survey in the Mediterranean area following a review of the papers published until now.

## 2. The Geoswim approach

The surveys were carried out along lengthy sectors of rocky coasts, up to 14 km per day (see Table in Additional materials), and were carried out following a protocol described by [Furlani \(2020\)](#). It consists in coastal surveys of selected sectors of rocky shoreline, mainly plunging cliffs or sloping coasts (sensu [Biolchi et al., 2016a, 2016b](#)), with specific observations of lateral changes in coastal landforms, such as tidal notches, presence/absence of submarine freshwater springs, ecological observations, such as presence/absence of barnacles, limpets, wormshells and various red algae. Alongside the observation and measurement of the aforementioned coastal features, instrumental data, such as time-lapse images of the stretch of coast being surveyed, images to document relevant landforms or other prominent objects, videos to document the overall survey, physical/chemical parameters to localise submerged freshwater springs and bathymetric measurements to define the depth at the cliff bottom or to produce transects perpendicular to the coast are all collected.

Survey activities are carried out either by single surveyor or usually by a team of snorkel surveyors and assistants, averaging 5/6 persons (see Tables in Additional materials). No type of engine is used on the raft



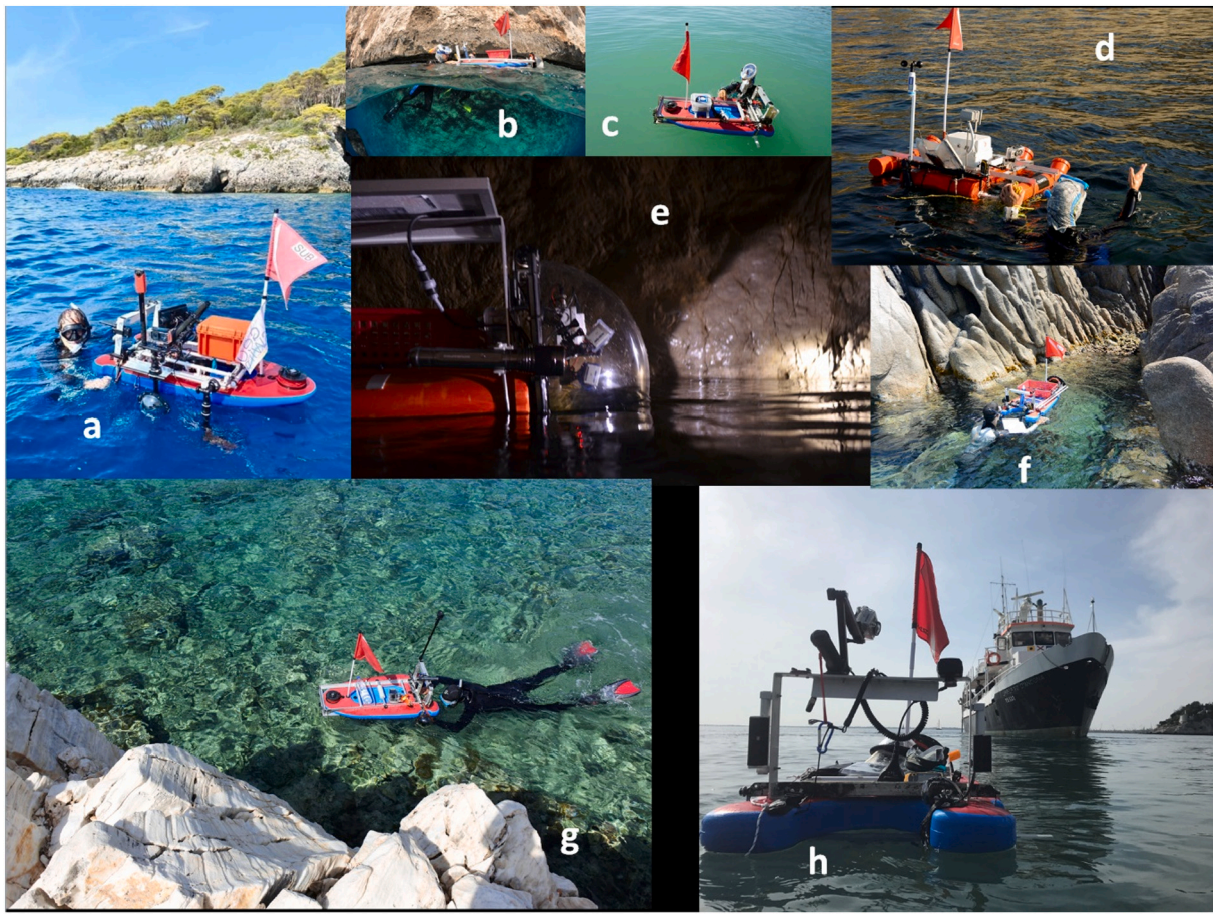


**Fig. 2.** The ISR used during the snorkel surveys; a) the latest version of the ISR used in 2020 around the Tremiti Islands (Adriatic Sea, Italy); b) the ISR used in 2015 around Tavolara island (Sardinia, western Mediterranean); c) the ISR used in the Gulf of Trieste (Italy) during the field test; d, e) the ISR used during the 2013 campaign around Gozo island (Malta); f) the raft used in 2015 around the island of Ustica; g) the version of the ISR used in 2017 around Paros in Greece; h) the ISR and the support boat used during a field test in the Gulf of Trieste (Italy) in 2017.

during the snorkel surveys.

The tools and instruments used for the swim surveys is described in [Table 1](#) and discussed in detail by [Furlani \(2020\)](#). The instruments, such as GPS, cameras, CTD sensors, echosounder etc. are fixed onto a specially-built raft (ISR, [Fig. 2](#)). Depending on the goals of the expedition, all the instruments, or a part of them, can be fixed at the raft ([Fig. 2](#)). One or more cameras can be set in waterproof housings, and allow the collection of ongoing videos and time-lapse images of the coastline being surveyed. The cameras should be set laterally with respect to the raft in order to collect time-lapse images every second, or less, in the direction of navigation. The cameras set below the waterline include a plastic dome 6 in. in diameter in order to perform with superior optical performance in the seawater ([Fig. 3](#)). In the dome fixed in the bow ([Fig. 2](#)), the cameras can collect videos above and below the waterline simultaneously thanks to the geometry of the lens itself. These are used to document the field surveys ([Figs. 1, 7, 9, 10, 12, 13, 14 and 16](#)).

Regarding the DAQ (data acquisition) system, each device is autonomous with respect to the other. The synchronization of data collected during each surveying day is carried out with respect to the Coordinate

Universal Time (UTC) and the comparison with GPS coordinates.

The surveys follow a predetermined route at roughly 1 m to 5 m from the coastline in order to identify the lateral variations in the coastal geotargets, and at the same time collect time-lapse images above, below and at the waterline. Small changes in the route can occur with respect to the planned one due to the local topography or due to worsening weather and sea conditions.

Observations are usually reported via radio to the support boat and written in the field booklet. The latter also includes other navigational information, such as the start point, end point, changes in swimming direction, etc. Waypoints or geotags are also sometimes documented by single point images.

Scuba dives have been used to collect data in specific situations, such as surveys of submerged sea caves or archaeological remains. More frequently, geomorphological, archaeological and paleontological observations have been carried out up to 25–30 m above sea level.

Beside field data, we also collect old images, postcards, and private photos, in order to compare the survey data providing the current topography with past topography obtained from old images.



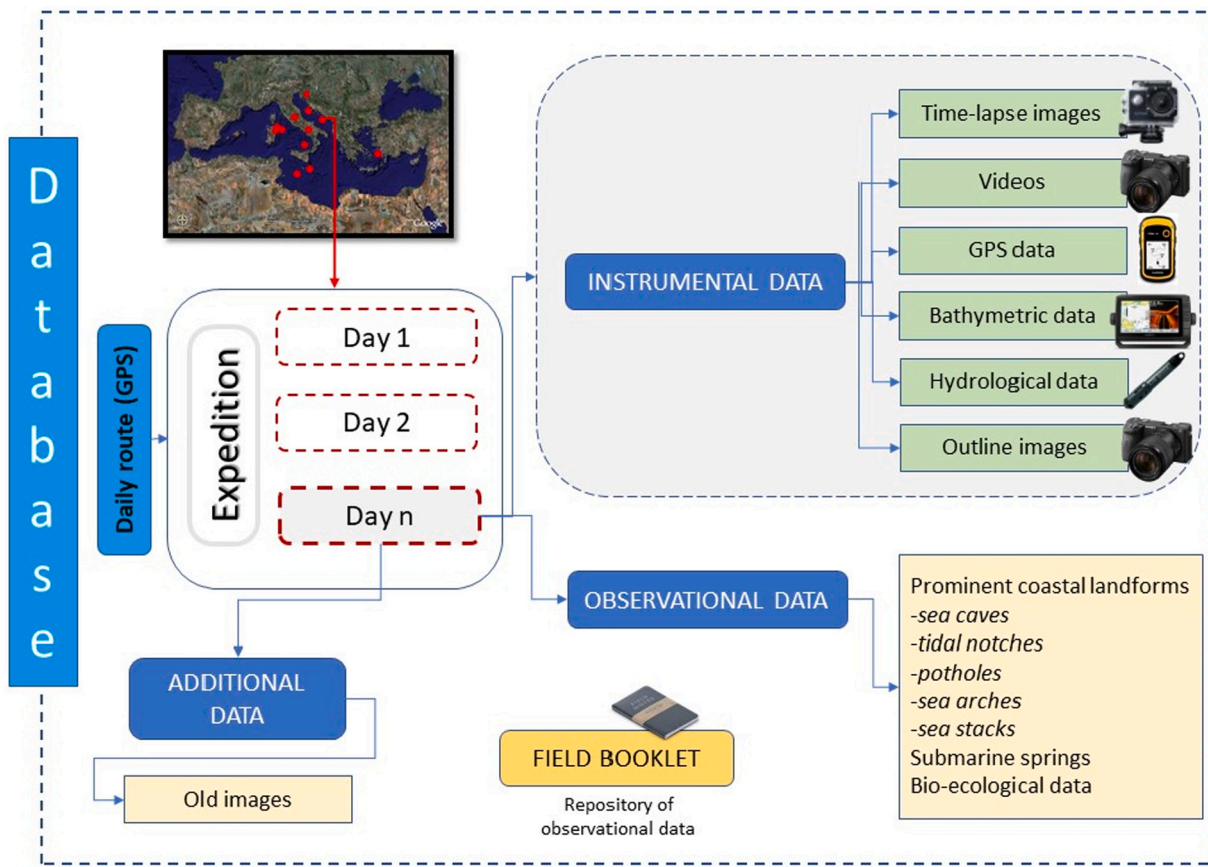


Fig. 3. Diagram of the Geoswim archive.

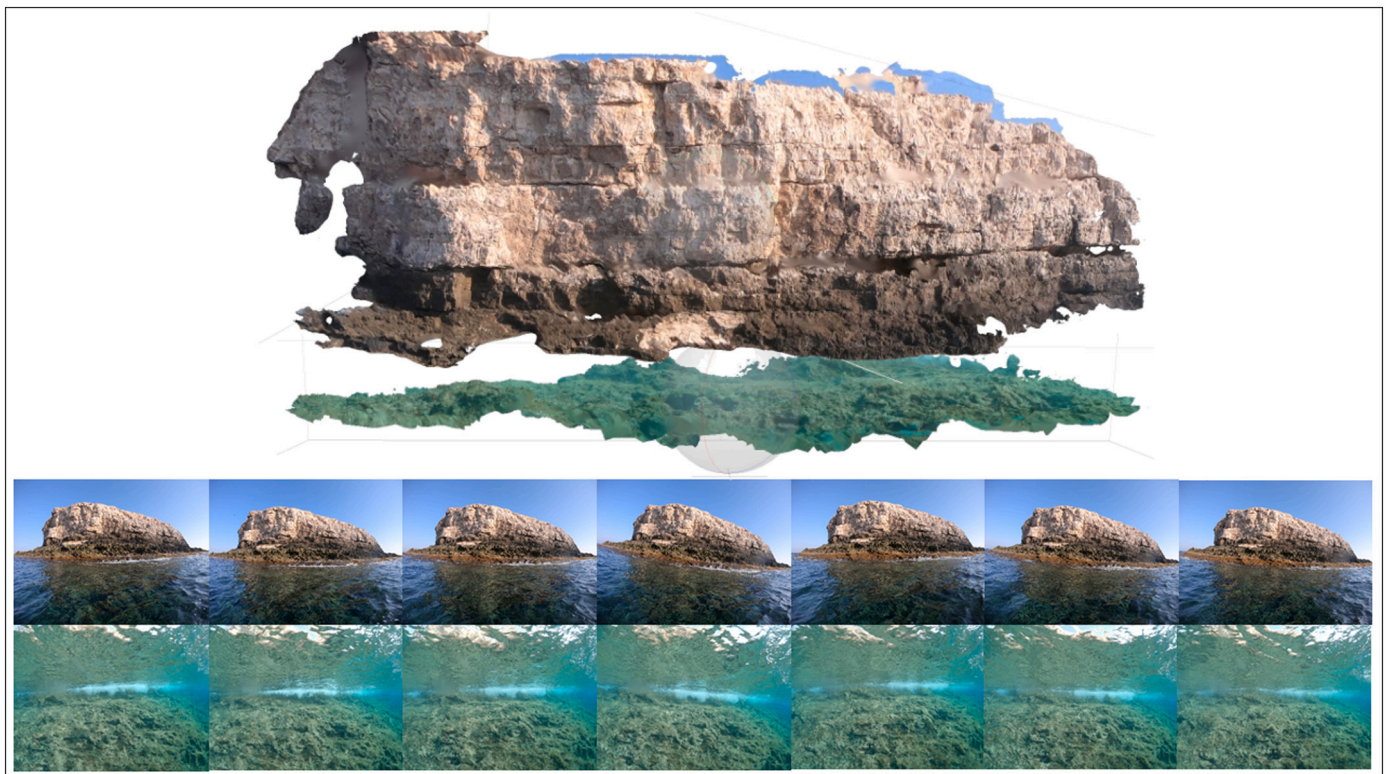
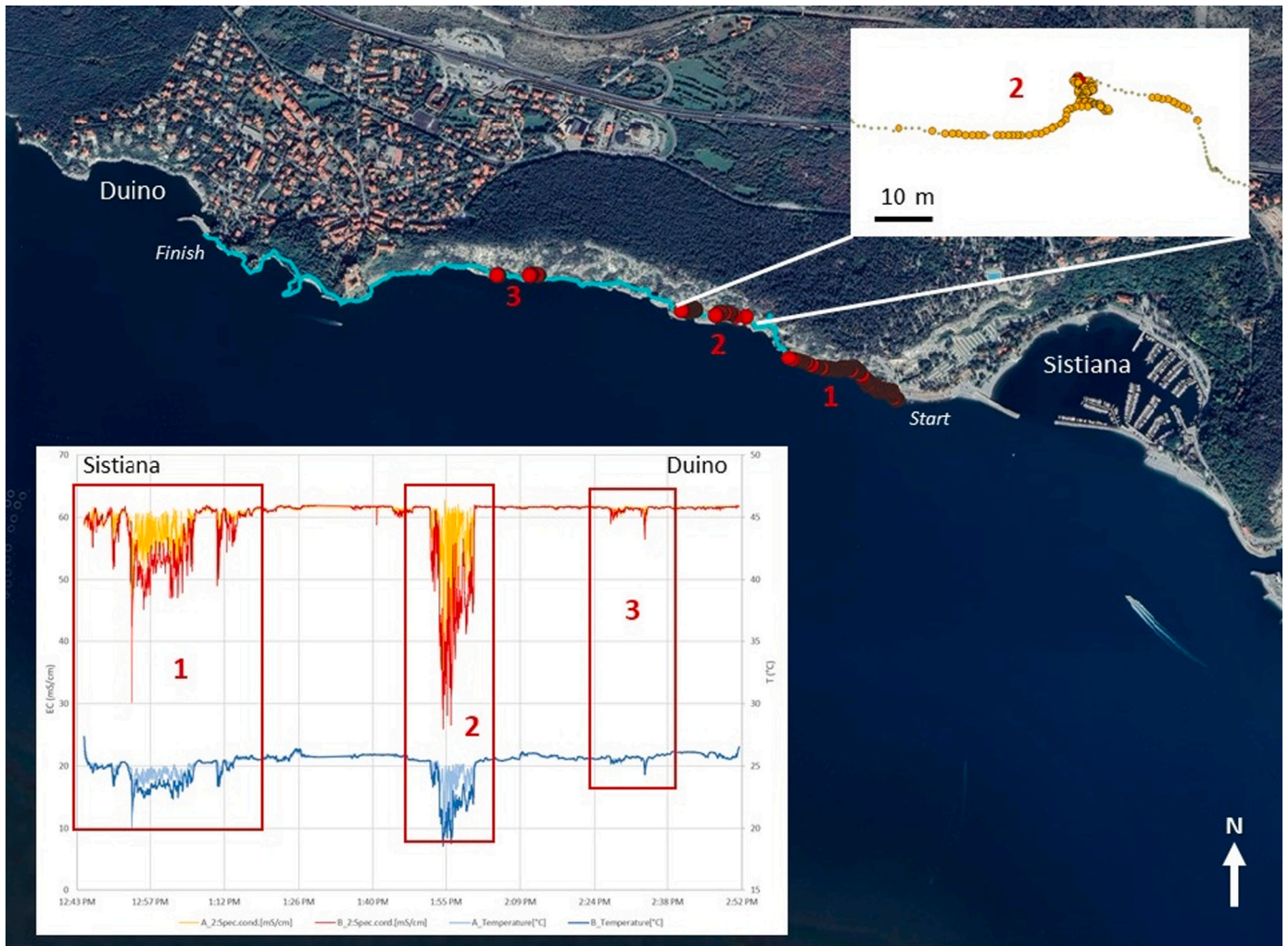


Fig. 4. Building of 3D models of a short sector of plunging cliff on Lampione Island (Sicily, Italy) above and below the waterline from sequence of time-lapse images collected every 0.5 s. A selection of these images is reported below.



**Fig. 5.** EC and T log acquired in the sector between Sistiana and Duino (Gulf of Trieste, Italy). The red circles represent the T and EC anomalies corresponding to submarine springs. In the lower left pane a graph with T and EC values collected in the field is reported, while in the upper right pane a detail of the 2nd area is given. The red circle represent the minimum values of EC, corresponding to a small spring with a large submarine outflow. (For interpretation of the references to colour in this figure legend, the reader is referred to the web version of this article.)

### 3. Data

The geometry of the database that includes time-lapse images, outline images and videos of the tidal and nearshore zone together with hydrological data, such as temperature and electrical conductivity, and observational data for use in coastal studies is presented. All field data are organized into folders on the basis of the survey day. A code is given to each surveying day and corresponds to a folder. Each folder is organized as shown in Fig. 3. In the following paragraphs, the type, amount and resolution of data collected are described. In the Table reported in “additional material” we also added the parameters of each day of survey and the related data. Data are stored on a dedicated server in the University of Trieste.

Data are divided respectively into (1) instrumental data (IS) collected in continuous form during the survey, (2) observational data (OS), which are usually collected at prominent sites, and additional data (AD), such as old images of the surveyed coast that are mainly drawn from the web and in local historical and photographic books. In the

following two paragraphs we describe the data collected in detail. The amount of data, its resolution as well as the type of data are gathered with the aim of ongoing improvement, mainly due to the continuous improvement of technology.

The quality of data collected during the expeditions is reported in the Table in additional material. In particular, the resolution of images has improved over the years because cameras have been changed, as specified in the table following technological improvements in their function and the introduction of mirrorless cameras.

The database is extensively described in the following paragraphs.

Data collected during 20 expeditions along 535.3 km of shoreline from 2012 to 2022 is described in Table 2.

#### 3.1. Instrumental data

Videos and images were used for different aims, as summarized by Furlani (2020), in particular, for 3D modelling, the creation of a baseline survey archive, identification of coastal landforms or marine deposits,



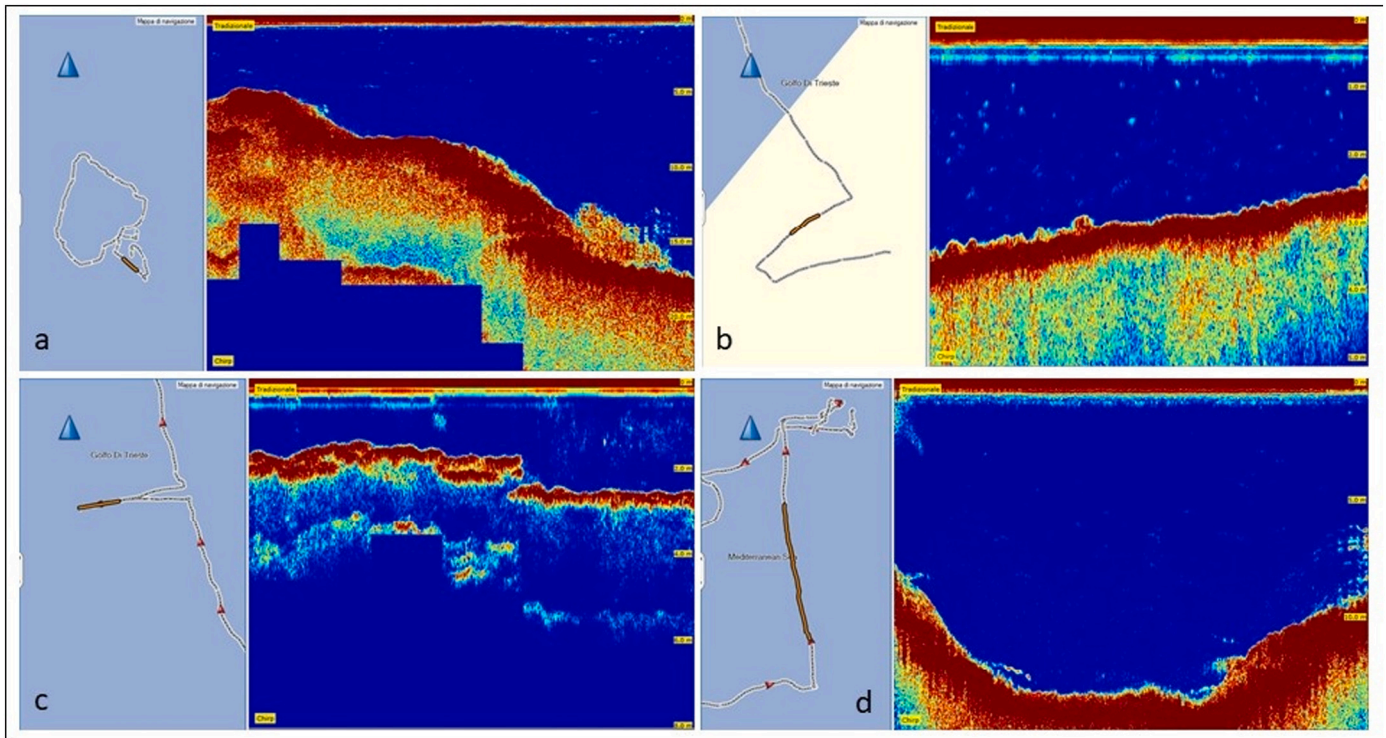


**Fig. 6.** Some Example of sonar profiles collected with a Garmin Echomap Plus 62cv; a) Profile along a profile at the southeastern sector of the island of Lampione (Pelagie Islands, Sicily, Italy); b, c) profile perpendicular to the coastline at Punta Sottile (Muggia, Gulf of Trieste, Italy). In c, a submerged Roman Age dock was surveyed; d) profile at the entrance of Cala Uccello (Lampedusa island, Sicily, Italy).

etc. (e.g. [Biolchi et al., 2020](#)).

The approach to collecting images follows the procedures used within the Geoswim programme ([Furlani, 2012](#); [Furlani et al., 2014b](#); [Furlani, 2020](#); [Furlani et al., 2017a, 2017b, 2018, 2021b](#)). It aims to collect data along rocky coasts, in particular around the tidal zone. Data are collected using cameras and other instruments hosted on a small raft ([Fig. 2](#)) adapted to float parallel to the coast. The operators push the boat to navigate at a constant distance from the coast, ranging from 1 m to 15 m, depending on the local topography.

Images of the intertidal zone are collected using the action or mirrorless cameras installed both above and below the waterline. The former are positioned at an elevation ranging from 0.5 m to 1 m above the waterline, while the others are positioned 0.5 m below it. Moreover, a camera is installed inside a dome at the bow, in order to document the surveying operations with video ([Fig. 3](#)). GoPROs are set in time-lapse mode in order to collect one photo per second and record wide sectors of rocky coast in detail. Images are then downloaded to a database that gathers images of all the expeditions.

### 3.1.1. Time-lapse images

Time-lapse images were collected from the fifth expedition onwards, carried out in 2015 at Malta ([Table 1](#)). Between 2015 and 2017 images were collected every 1 s, while from 2018 they have been collected every 0.5 s because a higher number of images allows for better resolution when 3D modelling. The archive here presented holds hundred thousand of time-lapse images, in particular 396,444 collected above the waterline, and 190,531 collected below the waterline. Time-lapse images have been collected since 2015 using a single camera at the

waterline, while from 2018 two or more cameras have been set both above and below the water level (see Tab. In Supplementary materials).

[Furlani et al. \(2020\)](#) discussed the possibility to build 3D models of selected sectors of coastline and showed that horizontal time-lapse images are particularly useful on plunging cliffs because cameras are perpendicular to the sea cliffs and images are collected closer to the wall. An example of 3D model of the cliff is reported in [Fig. 4](#).

### 3.1.2. GPS data

The GPS data are saved in .gpx format. The route of the survey is divided into roughly one file per day. At the beginning of the project, from 2012 to 2016, a position coordinate was taken every 30 s. Then this was increased to a position coordinate per second to compare it with the multiparameter probe data and outline images. Other GPS data have also been collected, starting from 2017, from the action cameras and echosounder that have integrated GPS.

The total length of the coasts investigated with the Geoswim approach amounts to 541.8 km, while 24 km have been re-surveyed for tests or to obtain further data. The total length of survey is 559.5 km, covered in 339 h and 42 min of swimming and a mean value of 4:13 h per day. The length of some sectors have been estimated in case of GPS malfunction.

### 3.1.3. Videos

Videos were recorded above and below the waterline during the 2012 and 2013 campaigns. From 2014, a dome set in the bow of the raft was added in order to frame both above and below the waterline. Moreover, the cameras were fixed to a gimbal in order to stabilize the



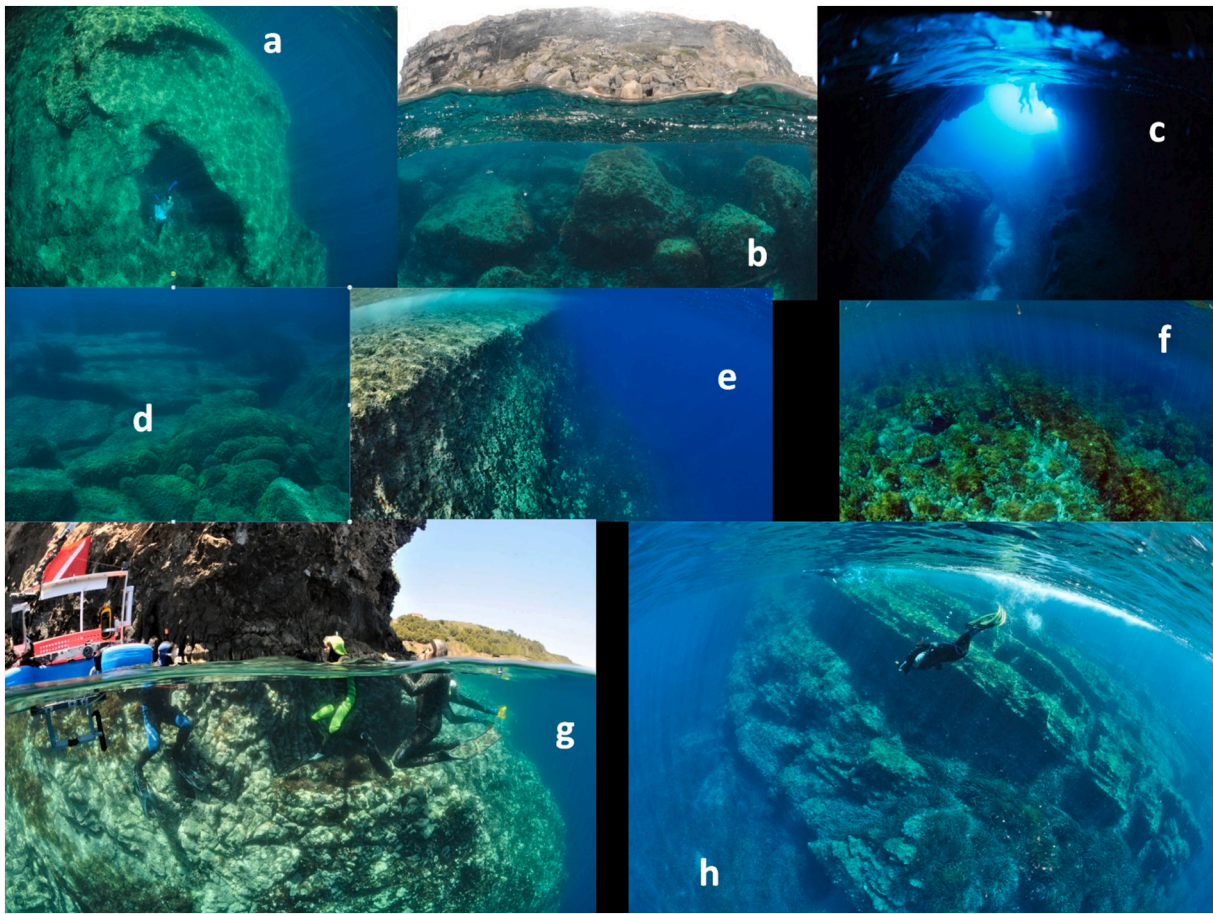


**Fig. 7.** Outline images of coastal objects: a) submerged “tafone” at –10 m bsl at Tavolara, Sardinia, Italy; b) submerged collapsed blocks at Favignana, Egadi islands, Sicily, Italy; c) the submerged part of a sea cave at Marettimo, Egadi islands, Sicily, Italy; d) beachrock up to 40 cm in thickness at Tavolara island; e) a platform with *Lithophyllum* sp. at Ustica island, Sicily, Italy; f) a submerged dyke at Ustica island; g) a u-shape landform carved in a carbonatic inclusion in volcanic rocks at Ustica island; h) submerged limestone beds at Marettimo, Sicily, Italy.

images when the raft tilts, pans and rolls. From 2015 to 2017, only images with the camera within the dome were collected. Videos are now used only as support for the post-processing of instrumental and observational data. Since 2020, 360 videos above the waterline have been collected, while from 2021 these were also taken below the waterline.

#### 3.1.4. Hydrogeological data

Variations in sea water temperature (T) and electrical conductivity (EC) are due to the presence of freshwater outflow of small rivers, or to the presence of submarine springs, the latter in particular along carbonate rock coasts. Some local variations may be due to human activities, such as water discharges (water purification plants, sewer discharges, swimming pools or tourist facilities along the coast, etc).

Continuous measurements allow the precise mapping of the location of submarine springs along wide transects of surveyed coasts, as shown by Furlani et al. (2014b) and Furlani et al. (2017b). Physical/chemical parameters are strongly influenced by rainfall before the surveying period (Furlani et al., 2014b) so, depending on the period, some springs may have no freshwater runoff into the sea. Furlani et al. (2014b)

suggested a significant correlation between the position of submarine springs and submerged tidal notches in the northern Adriatic Sea, while it was not observed in other areas of the Mediterranean Sea, despite having the presence of marine notches and underwater springs.

EC and T have been collected during 86 surveying days. No data was collected only during photographic equipment testing campaigns.

#### 3.1.5. Depth data

Depth information is collected both from puntiform measurements at prominent sites and collected with a sonar Chirp mounted on the raft. Depth information is collected, for example, at the entrance to sea caves in order to characterize their entrances and the ratio between the emergent and submerged part (Fig. 5), at the top and base of archaeological remains, or to measure the depth of potholes, etc.

From 2015, depth transects perpendicular to the coastline have been collected to characterize the submerged part of the coast. Depth measures are collected using a portable hand echosounder every five fins. From 2017, continuous profiles parallel to the coastline have been collected with the Chirp sonar. Until now, 48.6 km of profiles have been acquired. At prominent sites, sonar profiles perpendicular to the

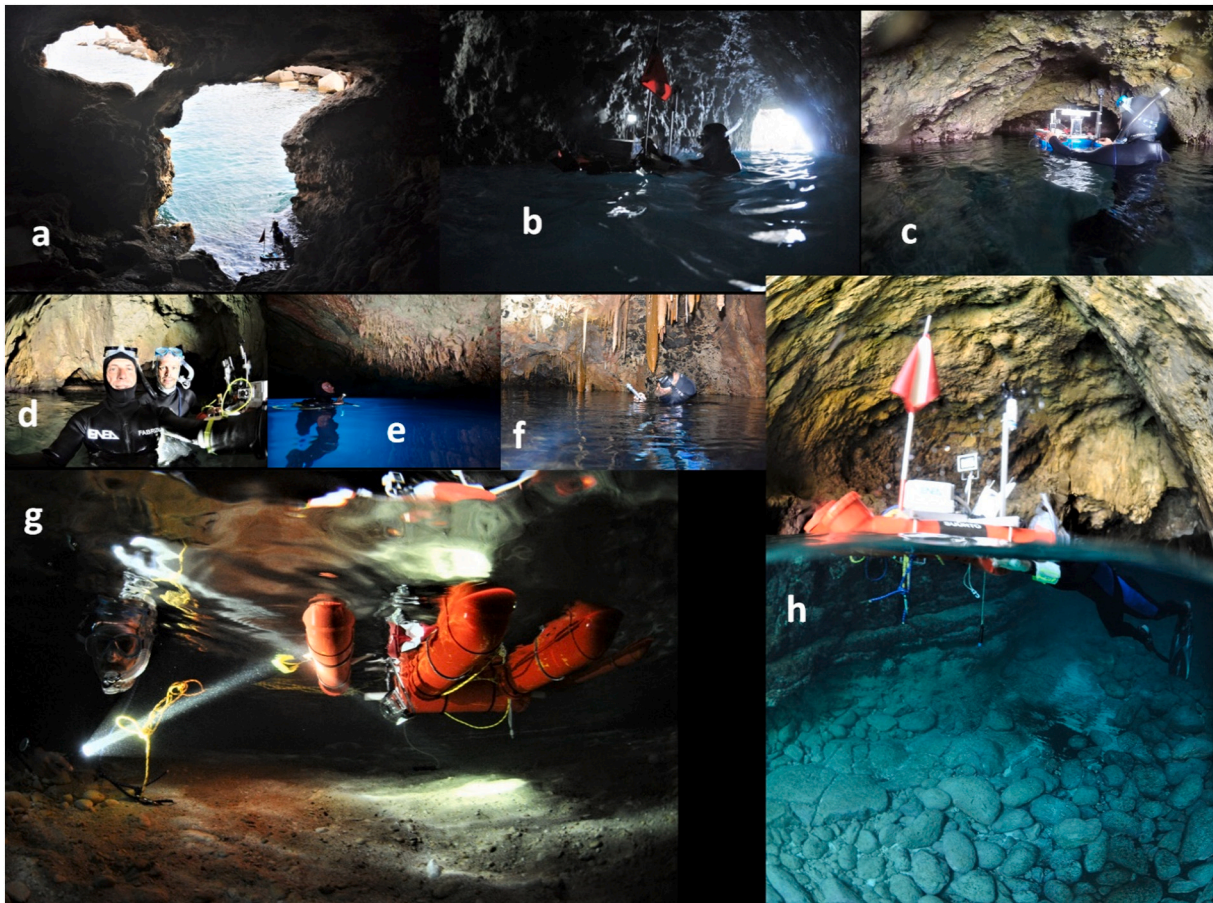


**Fig. 8.** Collage of sea caves mapped in the studied sectors: a) exploring a marine cave near Palermo town, Sicily; B) exploring a marine cave on Gozo, Malta; c and d) exploring a marine cave on Comino, Malta; e) exploring a marine cave on Paros, containing speleothems, Greece; f) exploring a marine cave on Ustica, containing speleothems with marine layers, Ustica; g and h) sea caves on the southern coast of Gozo, Malta.

coastline are also collected (Fig. 6).

### 3.1.6. Outline images of prominent coastal objects

During the surveys, the teams, both swimming and support, usually collect additional outline images to document the general features of the observational data items previously described. Outline images are collected using several different cameras and, when available, with GPS position. These images can also be used to reconstruct the position of coastal landforms in case of georeferencing issues, to have additional views of the same object, or to add information to time-lapse images.

So far, 15,240 outline images have been collected during the Geoswim expeditions.

## 3.2. Observational data

Alongside the data described above, collected continuously during the swim surveys, the team also collects observational data, i.e. precise or extensive observations or additional measurements on specific objects such as caves that develop above sea level, marine furrows, prominent coastal landforms, the presence of underwater springs or bio-ecological observations. The geographical position of these objects and a collection of a number of outline images represent the minimum

information collected during the survey of these kind of data.

A list of the type of observational data is reported in Furlani (2020) and Furlani et al. (2021b). Observational data are here divided in (1) prominent coastal landforms, (2) underwater springs, (3) bio-ecological observations, and (4) archaeological data.

### 3.2.1. Prominent coastal landforms

Prominent coastal landforms are, in this case, considered to be stacks, sea caves, sea arches, and other landforms developing along the coast which can be identified, delineated and possibly measured. Coastal landforms of rocky coasts are mainly generated by erosion processes. They exhibit distinctly different shapes depending on the type of dominant process and the environmental and lithological conditions.

**3.2.1.1. Sea caves.** A census of sea caves that develop at the present sea level was also carried out. The number of sea caves per surveying day is reported in the Table in Supplementary Materials. Roofless caves are numbered separately. Usually, alongside the geographical position, additional data are collected, including their size and morphometric parameters, their position with respect to the present-day sea level, the nature of the seabed within them, such as sandy or rocky, and the occurrence of any beaches in the innermost part of the caves. Some caves



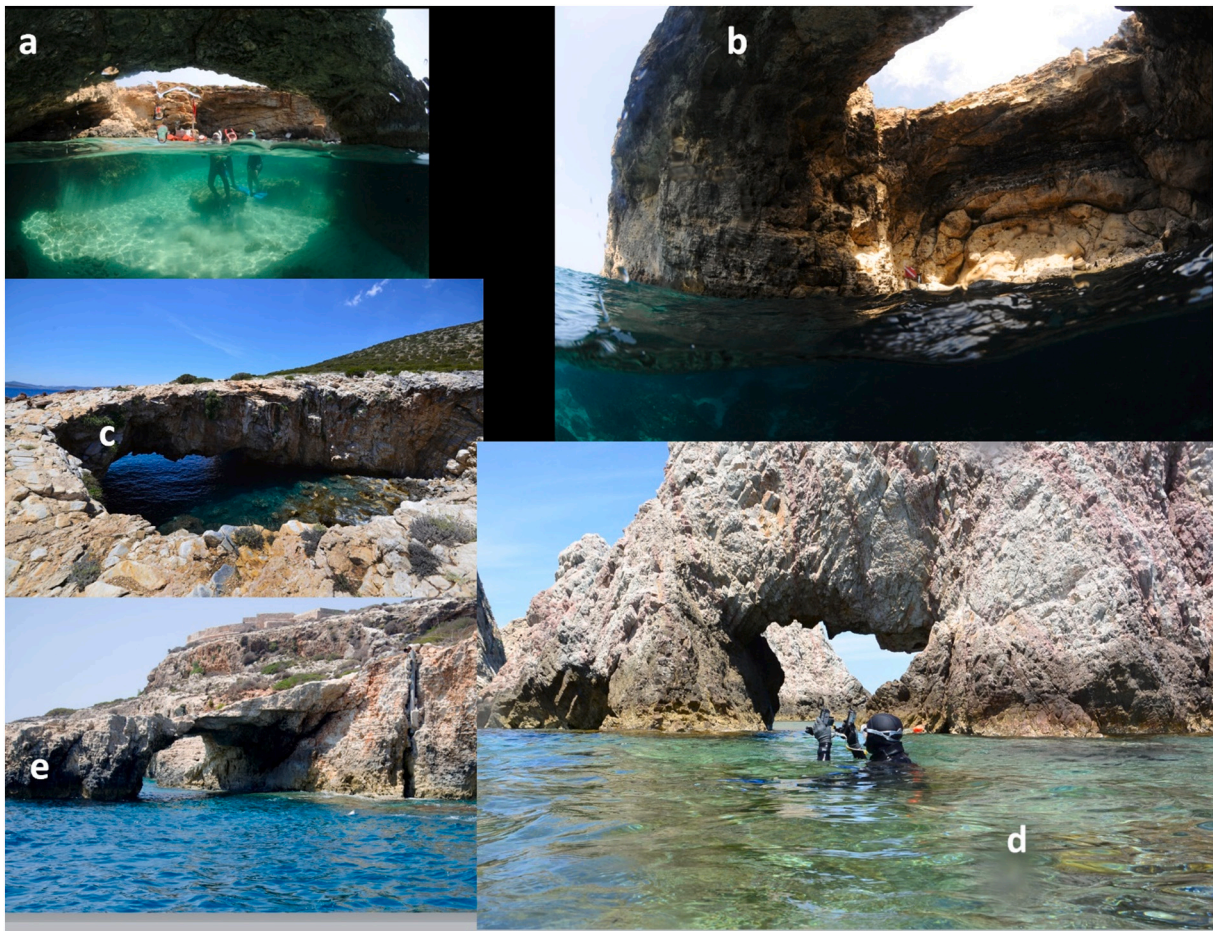


**Fig. 9.** Collage of sea arches surveyed in the studied sectors of rocky coast: a-c) sea arches on Gozo, Malta, in correspondence of roofless caves; d and e) sea arches on Paros, Greece.

may be the result of the coalescence of multiple caves and complex shapes may result (Fig. 8).

Thus far, 268 sea caves have been located, registered and measured during the expedition (Table in supplementary materials). Eight of them are roofless caves. Their abundance mainly depends on the lithological features of the surveyed sites. Maximum frequency of sea caves per kilometer has been surveyed at the Ansedonia promontory (see Tab. In Supplementary materials) and the promontory of Gaeta. Also some sector of the island of Lampedusa show high values of frequency.

At Egadi island, an unknown sea cave was discovered at 500 m from the main harbour of the island, in fact it is not included in the local cadaster of sea caves (Miragoli, 1994). As reported by Furlani et al. (2021b), the cave was called Geoswim. It is characterized by an entrance of less than 1 m in height asl and the sea bottom lays at about 2 m bsl. Within the cave, three corridors, each of them parallel to each other and to the coastline, elongate for about 70 m each one. They end with three small gravel beaches. The cave was recently used to install photo traps to survey the presence of the monk seal by the Italian Geological Survey.

**3.2.1.2. Sea stacks and sea arches.** Erosion along rocky coasts occurs at various rates and is dependent both on the rock type and on the wave energy at a particular site. As a result of the above-mentioned

conditions, wave-cut platforms may be incomplete, with erosional remnants on the horizontal wave-cut surface. These remnants are called sea stacks, and they provide a spectacular type of coastal landform. Some are many metres high and form isolated pinnacles on the otherwise smooth wave-cut surface. Because erosion is a continual process, these features are not permanent and will eventually be eroded, leaving no trace of their existence. The number of sea arches and sea stacks per surveying day is reported in the Table in Supplementary Materials.

Another spectacular type of erosional landform is the sea arch, which forms as the result of different rates of erosion typically due to the varied resistance of bedrock. These archways may have an arcuate or rectangular shape, with the opening extending below water level. The height of an arch may be up to tens of metres above sea level.

Along the surveyed coasts, we mapped 11 sea arches and 14 sea stacks. The sea arch at Gozo, also known as Azure Window collapsed in March 2017 after a severe storm.

**3.2.1.3. Marine notches.** The occurrence of modern (MTN) and MIS 5.5 tidal notches (FTN) have been observed and delineated in the surveyed areas, the lateral extension of the tidal notches being quantified from time-lapse images, while field measurements have been collected at selected sites, where the surveyor assumes that information is more



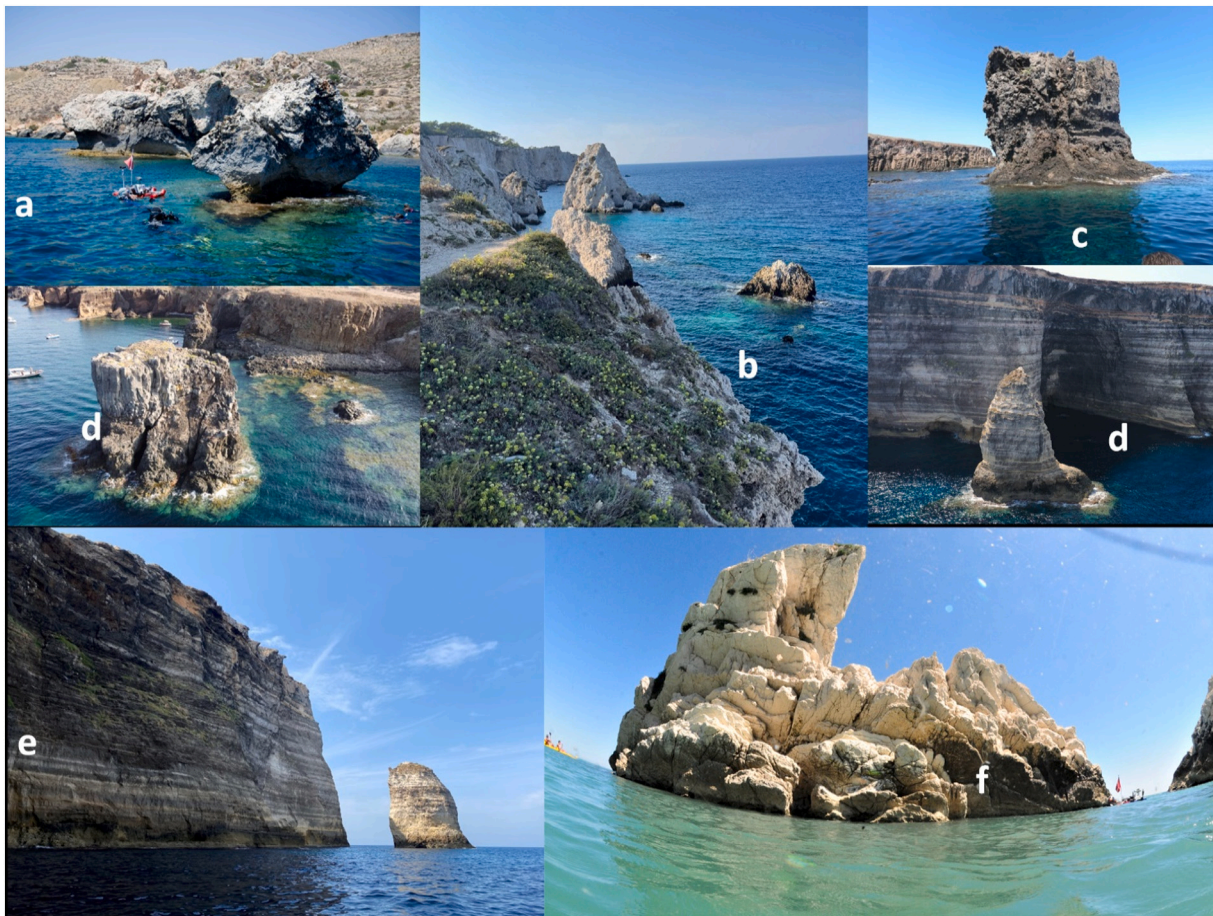


**Fig. 10.** Collage of sea stacks surveyed in the studied sectors of rocky coast: a) sea stack on Gozo, Malta; b) sea stacks on the Tremiti islands, Puglia, Italy; c and d) the sea stacks along the northern coast of Ustica, Sicily, Italy; e and f) sea stack on Lampedusa, Sicily, Italy; g) sea stack at Monte Conero, Marche, Italy.

meaningful and representative of the general aspect of local tidal notches. In particular, data are collected following the approach proposed by Antonoli et al. (2015) measuring their depth, width and height (Fig. 11). Submerged tidal notches, sometimes more than 20 m in depth, have also been surveyed on the sidelines of the project (Antonoli et al., 2017). Their occurrence depends on the lithological features of the surveyed sites, since there are very common on Mesozoic and Tertiary carbonates, but have also been observed for the first time on volcanic rocks on Ustica (Furlani et al., 2017a).

Furlani et al. (2021b) reported the presence of 47,387 m of MTN and 603 m of FTN along the rocky coasts of the areas which can be considered tectonically stable and pointed out that with respect to the total length of surveyed coast, the occurrence of tidal notches accounts for 85 % of the modern coastline, and only 1 % of the MIS 5.5 equivalent. Therefore, only 1 % of the surveyed coast showed the presence of fossil markers of paleo sea levels above the datum. They have attributed this difference to erosion processes occurred from 125 ka to nowadays that did not allow the preservation of the evidence of past sea level stands.

In the Table in Supplementary Materials, marine notches are reported as presence/absence in the surveying day. In particular, marine notches have been found during 54 surveying days.

**3.2.1.4. Potholes.** Potholes, are roughly circular- or bowl-shaped depressions worn by the grinding abrasion of clasts rotated under the energy

of moving water on the seabed (Sunamura, 1992). Sometimes they can be elongated in shape because of the coalescence of neighbouring potholes or the rock's hardness (Trenhaile, 1987).

These were encountered in almost all the exposed sectors of coast surveyed during the Geoswim expeditions. The location of pothole networks or single units were recorded in the field booklet and photographed. In the Table under Supplementary Materials, potholes are reported as presence/absence on the surveying day. In particular, potholes have been reported during 35 surveying days.

### 3.2.2. Underwater springs

Underwater springs are freshwater sources leaking from the submerged bedrock or as sieves with widespread holes on sandy and rocky sea beds. These may be both permanent or temporary. They form in Karst areas where, during the last marine ingressions, the sea level rose, or the shoreline lowered, leaving carbonate rocks with freshwater beneath the waterline. The hydrostatic pressure related to these springs may be very high with the freshwater emerging at the sea surface producing a sort of boiling effect. This 'boiling' is very visible when the springs are sink-like and the water comes from large submerged holes, as in many cases along the Eastern Adriatic coast. At the springs, transparency is lowered and the water is much colder. The delineation of these springs is achieved through the perception on the skin of differing water temperatures. The position and any additional temperature



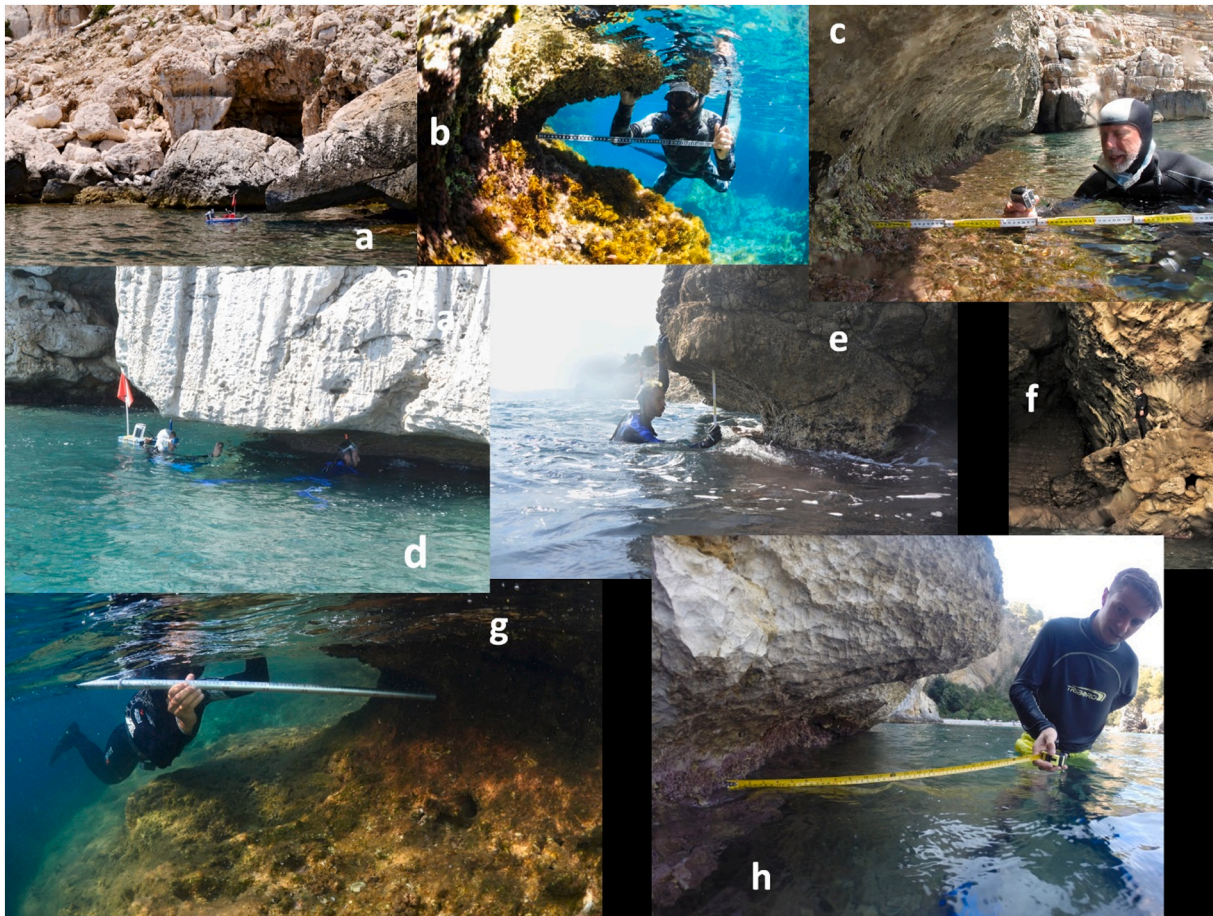


**Fig. 11.** Tidal notches: a) fossil tidal notch at Tavolara, Sardinia; b) submerged tidal notch at about – 45 cm, Paros, Greece; c) measuring a present-day tidal notch with a *Lithophyllum* sp. platform at Punta Giglio (Capo Caccia, Sardinia); d) present-day tidal notch with a *Lithophyllum* sp. platform at Punta Giglio (Capo Caccia, Sardinia); e) measuring a present-day tidal notch with a Vermetid platform at its base (near Palermo, Sicily); f) measuring a MIS 5.5 tidal notch at 5.5 m asl at Gaeta (Italy) carved in conglomerates; g) measuring a present-day tidal notch on the southern coast of Lampedusa, Sicily. The notch seem to be slowly sumberging in the inner portion of an inlet, as also observed in southern France (Antonioli et al., 2017); h) measuring the present tidal notch at Palinuro, Campania.

measurements are performed by the snorkelers. During winter, these springs have a more intense water flow due to heavy rainfalls. This causes strong currents from the sea bed to the surface and around the springs. In the Table under Supplementary Materials, these springs are reported as presence/absence in the surveying day.

Areas with low values of EC and T were measured during 26 surveying days. A detailed analysis of these anomalies have been conducted by Furlani et al. (2014b, 2017b) in Istria and Gozo.

### 3.2.3. Bio-ecological observations

The bio-ecological observations performed as part of the Geoswim programme mainly relate to the intertidal zone, but occasionally observations are also conducted above and below.

In any case, generic observations are made on the presence / absence and possibly degree of coverage of certain organisms, such as limpets, barnacles, red algae, vermetids, etc. In the Table in Supplementary Materials, bio-ecological observations are reported as presence/absence in three separate columns for vermetids, *Lithophyllum* sp. algae, and *Patella ferruginea*, during the surveying day. Vermetid structures have been reported during 24 surveying days, while *Lythophyllum* sp. have

been reported during 41 surveying days. *Patella* sp. have been reported during 9 surveying days, in particular at Marettimo and northern Sardinia. De Sabata et al. (2015) reported for the first time an extended survey of the exact position of 200 *Patella* sp. along the coasts of northern Sardinia, as surveyed in the 2015 expedition.

### 3.2.4. Archaeological observations

The location, size and depth of archaeological and historical structures that are encountered along the route are collected during snorkel surveys together with a rough description of the artefact.

Usually, measures of the elevation above or below the sea level are collected at each site, also if already known, in order to compare them with published data. A new prehistoric deposit was discovered on the Ansedonia promontory during the 2017 campaign from about 2 m a.s.l. up (Fig. 15e).

In the Table in Supplementary Materials, archaeological objects are reported as presence/absence of observed objects on the surveying day.

We have found archaeological objects during 17 surveying days.



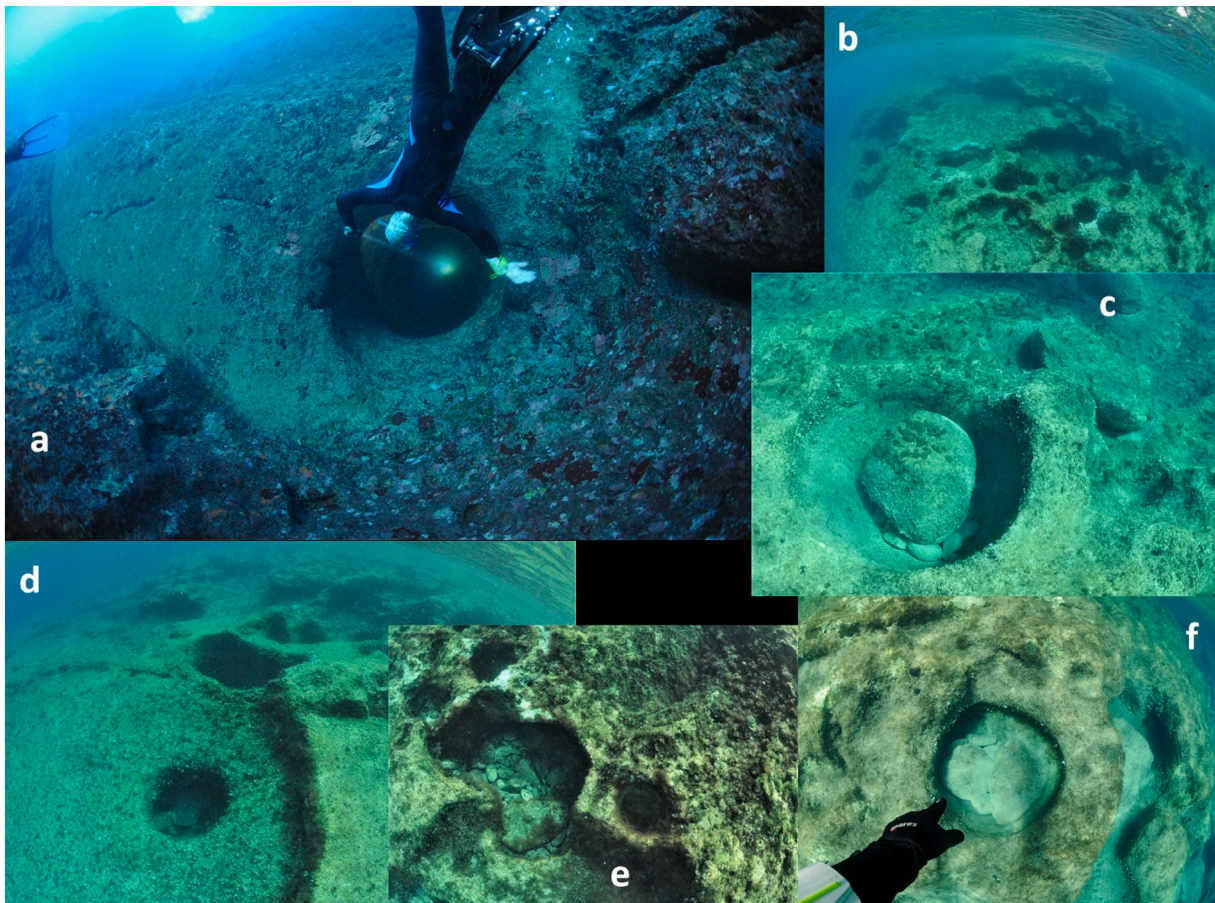


Fig. 12. Potholes surveyed during the Geoswim expeditions. A) Exploring a potholes at Capo Caccia at -5 m, Sardinia, Italy; b-f) potholes on Comino island, Malta.

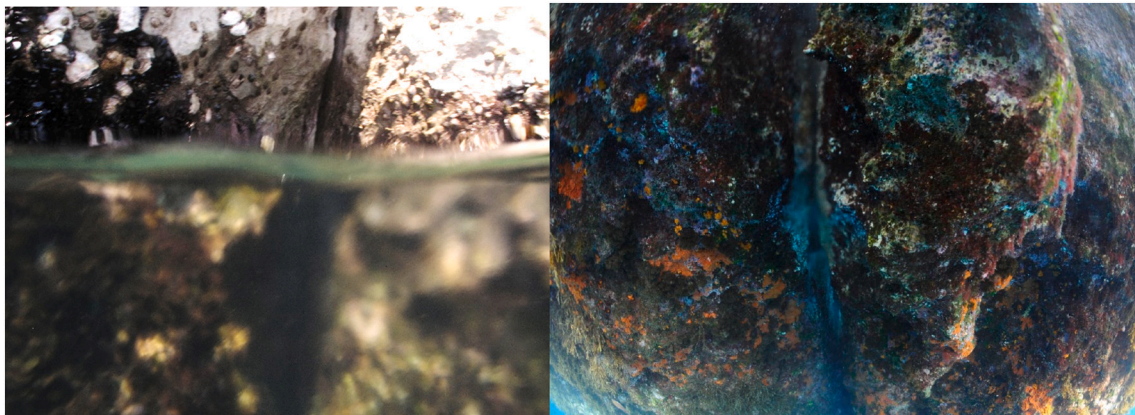


Fig. 13. Submarine springs in a) the Gulf of Trieste, Italy, and b) on Gozo island, Malta.

### 3.3. Additional data

Alongside the data described above, collected continuously during the swim surveys, the team also collects observational data, i.e. broad or narrow observations or additional measurements on specific objects such as caves that develop above sea level, marine furrows, prominent coastal landforms, the presence of underwater sources or bio-ecological observations. The geographical position of these objects represents the minimum information collected during the survey. A list of the nature and type of observational data is reported in [Furlani \(2020\)](#) and [Furlani et al. \(2021b\)](#).

#### 3.3.1. Old images

Old images of the surveyed stretches of coastline are stored in a separate folder within the main one ([Fig. 2](#)). At present 183 old images are stored, but additional photos are added when found (see the Table in Supplementary materials). The number of old images per surveying day is reported in the Table in Supplementary Materials. As an example, we reported a collection of images of the Duino (Gulf of Trieste) area.

## 4. Discussion

[Goudie \(1990\)](#) and [Dackombe and Gardiner \(1983\)](#) widely



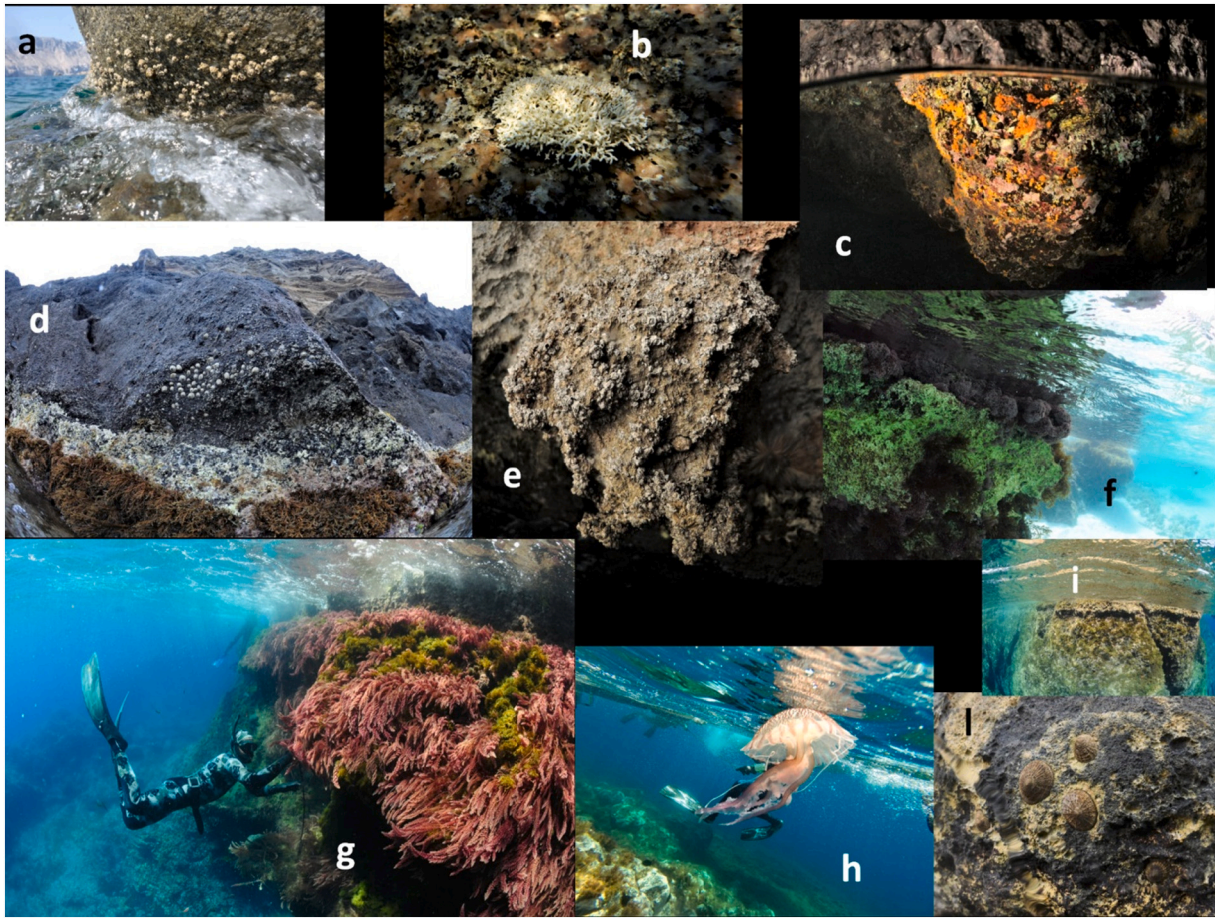


**Fig. 14.** Collection of images of biological objects: a) Chthamalids and *Phorcus turbinatus* (Molara Island (Sardinia, Italy); b) *Lithophyllum woelkerlingii* (Ustica island, Sicily, Italy); c) *Astroides calycularis* (Ustica, Sicily, Italy); d) Coralline encrusting and fucals (Ustica island, Sicily, Italy); e) Chthamalids (Tavolara island, Sardinia, Italy); f) *Corallina elongata* and *Jania rubens* (Paros island, Greece); g) Belt of *Asparagopsis taxiformis* and dictyotales (Paros island, Greece); h) *Pelagia noctiluca* (Ustica island, Sicily, Italy); i) belt with Corallineaceae and dictyotales (Ustica island, Sicily, Italy).

investigated the role and methods of terrestrial field surveying in geomorphology. It is the collection and gathering of data at the local level that represents a procedure carried out mainly through observation, measurement, sketching, etc. Snorkel surveys are a form of field survey. The approach proposed within the Geoswim programme is that of a research expedition from local to intercontinental in extent. Field surveys of rocky coasts had never been extensively carried out before Geoswim (e.g. Furlani, 2012; Furlani et al., 2014a), and there are still few examples of extensive surveys on rocky coasts. This is partly due to the hostile nature of rocky coasts, in particular plunging cliffs, the favorite morphotype within this programme. Starting from this consideration, the Geoswim programme the Geoswim program takes a significant value, being the only extensive swim-survey programme of rocky coasts.

The studied areas are mainly made of carbonate rocks (Furlani et al., 2021b). Igneous rocks coasts have been studied at Maddalena archipelago in northern Sardinia (Furlani et al., 2021b), while volcanic rocks at Ustica island (Furlani et al., 2017a) and recently at Ponza Island (Italy). Short sectors of the studied coasts are made of Quaternary deposits (Furlani et al., 2014b, 2021b) and terrigenous rocks (Furlani et al., 2014b). Usually, Geoswim campaigns investigate plunging cliffs and sloping coasts, because they are provide more reliable data for 3D modelling, as suggested by Furlani (2020). Moreover, these morphotypes allow to swim parallel to the coastline, as requested by the protocol (Furlani, 2020). On the contrary, shore platforms, low-lying rocky coasts, and screes do not permit to swim along straight routes because of topographical irregularities, such as submerged rocks or on the surface

of the water. The horizontal or sub-horizontal profile of the coast at the water level prevent the acquisition of horizontal images for 3D modelling. Anyway, observational data can be always be successfully collected on any type of coast.

Plunging cliffs are mainly developed on hard coasts, such as in carbonates or igneous rocks. Some examples of the former type occur at Istrian coasts, Gulf of Trieste, Gozitan and Maltese coasts, Capo Caccia, Tavolara island, the Tyrrhenian studied sites, and Capo Rama, while latter type occur at Ustica and Ponza island and in the Maddalena archipelago. The same for sloping coasts, which differ from plunging cliffs only for the lower sloping angle with respect to plunging cliffs (Biolchi et al., 2016a, 2016b). The angle of the slope mainly depends on the local structural setting and the type of outcropping rocks (Furlani et al., 2014a). Sectors with shore platforms were found in the Istrian peninsula and Gulf of Trieste on terrigenous coasts, and in some sectors of Maltese coasts at less resistant Globigerina limestone (Furlani et al., 2021b). Screes have been mainly studied at Gozo, small sectors of the northern coast of Malta, short sectors of the Ustican coast and Egadi islands. Pocket beaches are not considered rocky coasts, but are part of the rocky coastal system. The position of pocket beaches are usually reported in the log book.

The archive here presented holds hundred thousand of images, both time-lapse and outline, together with many hours of videos. These high-resolution images collected above and below the waterline allow to build detailed 3D models of the coastline and also to get a shot of the coast in the moment of the survey. Therefore potentially, the image dataset constitutes a very powerful archive for and to use the dataset as a



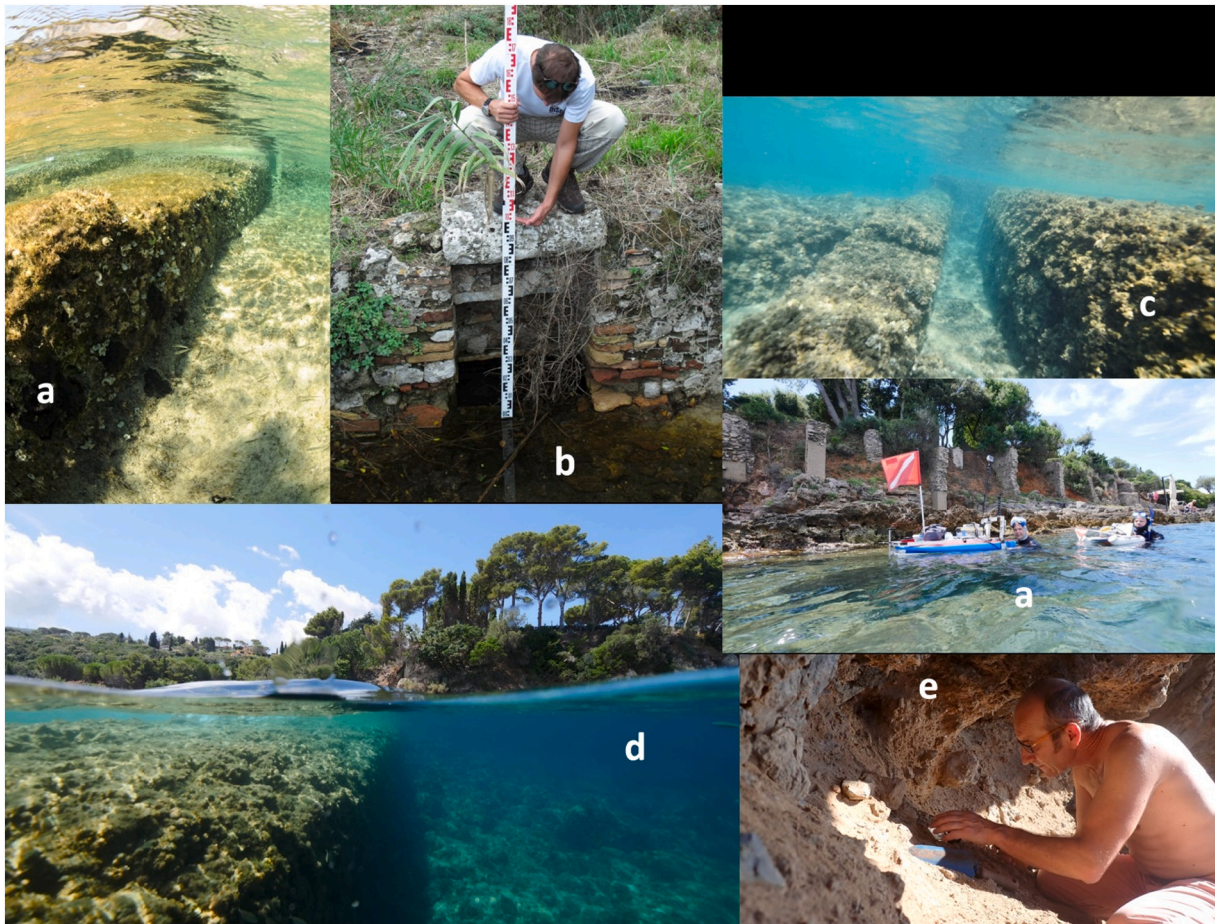


**Fig. 15.** Archaeological data; a, c archaeological remains at the Argentario promontory (Tuscany, Italy); b) measuring the elevation of Roman age fish tanks at San Felice Circeo (Lazio, Italy); d) exploring the Santa Liberata fish tanks at Porto Santo Stefano (Tuscany, Italy, dating to about 2 Ka BP); e) surveying of a prehistoric deposit discovered on the Ansedonia promontory in 2017 during the Geoswim campaign (Ansedonia, Tuscany, Italy).

baseline for future geomorphological and ecological comparisons. For example, [Biolchi et al. \(2019\)](#) used images taken from videos collected above the waterline to evaluate the movements of storm wave blocks in the southern sector of the Istrian Peninsula. Any repetition of the survey of selected sectors of coastline can be easily performed even by a single surveyor, as the observational data have already been collected in the mother campaign. Anyway, some sectors of Gulf of Trieste, the coastal area where the instrumentation usually housed, are repeatedly surveyed in order to test technology advancements of the ISR.

Regarding physical/chemical data, that are temperature and electrical conductivity, they are very useful in identifying underwater outflows of freshwater, as reported by [Furlani et al. \(2014a, 2017b\)](#). In particular, [Furlani et al. \(2017b\)](#) reported the location of all the submarine springs of the island of Gozo, in the Maltese archipelago. Although these submarine springs could also be identified with thermal satellite images or UAVs thermal images thanks to significant differences between sea and freshwater temperature ([Jou-Claus et al., 2021](#)), at certain times of the year, these differences in temperature are very low, so direct measurement of electrical conductivity allows for greater detail.

Observations collected during the expeditions have permitted the discovery of many new significant geomorphic objects along the coasts under investigation. They have in part already been published, such as the discovery of the Geoswim sea caves at Egadi island ([Furlani et al., 2021b](#)), or the precise mapping of the morphometric characteristics and extension of tidal notches in some tectonically stable areas in the Mediterranean Sea ([Furlani et al., 2021b](#)). The discovering of PTN in unforeseen contexts, such as on volcanic islands ([Furlani et al., 2017a, b](#)) or

in narrow inlets in a submerged position ([Antonioli et al., 2017](#)) have also been reported.

Significant contributions also concern, for example, the precise mapping of the Ribbed Mediterranean Limpet *Patella* sp. ([De Sabata et al., 2015](#)), very rare in the Mediterranean. [Bisanti et al. \(2022\)](#) published a paper regarding a local mass mortality of the Mediterranean orange coral *Astroides Calycularis* in the Pelagie Islands Marine Protected Area (Italy). The degree of the mortality impact at seven study sites of the archipelago (five within the Pelagie Islands Marine Protected Area) was quantified by estimating the proportion of affected colonies in populations of *A. calycularis*. The authors suggested that 2020 mortality event coincided with a longer lasting and warmer anomalous summer period, with sea surface water at the highest temperatures recorded in the last decade in the study area. Given the dramatic climatic predictions for the near future, [Bisanti et al. \(2022\)](#) suggested that new mortality events could occur, causing potentially new local extinctions.

During the Geoswim expedition at Favignana island in 2014 and at Ustica island in 2015, respectively one submerged speleotheme have been collected within respectively semi-submerged, and submerged sea caves. These data allowed to precisely define the Holocene transition from an emerged and submerged environment due to sea level rise ([Antonioli et al., 2021](#)).

A combination of observations and images were also used to study the geomorphic evolution of selected rocky coasts. In particular, the tectonic behavior and landslide evolution of the Conero area was studied thanks to PTN carved on collapsed blocks ([Furlani et al., 2018](#)). Comparisons were also made using old postcards and images collected in the study area.



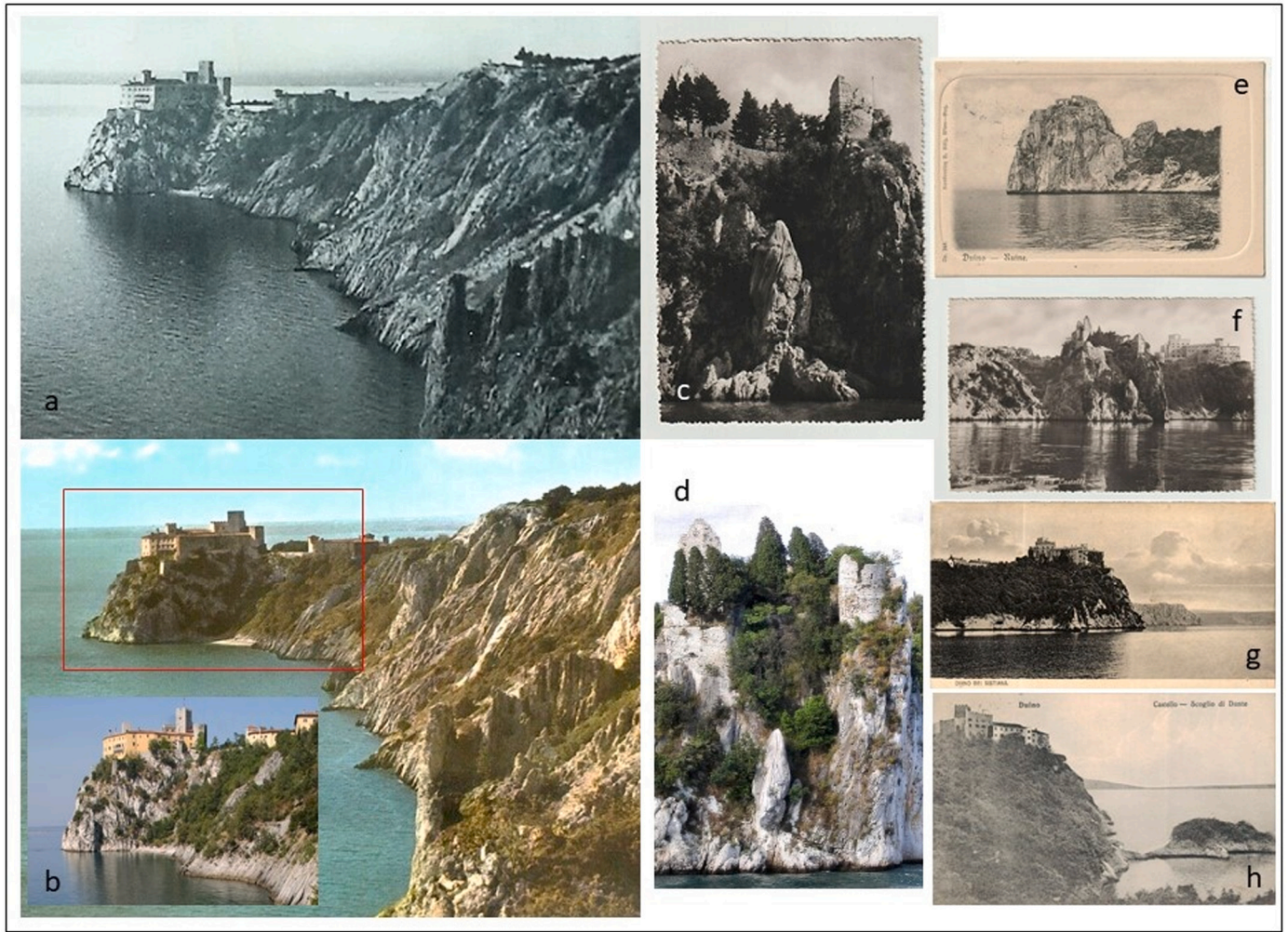


**Fig. 16.** Old images of the promontory of Duino castle (Gulf of Trieste, Italy); a) plunging cliffs at Duino in the 1950s from a postcard and b) the same area in the 1960s. Lower left, a zoom from a recent image of the castle; c and d) are the same locality respectively from an early 20th century postcard and a recent one; e to h) collection of postcards of the plunging cliffs below the old and new Duino castle.

## 5. Concluding remarks

Instrumental and observational data collected within the expeditions of the Geoswim programme in the Mediterranean area form a dataset composed of two sections. The first consists of digital images, videos, hydrogeological (T and EC) data, sonar profiles and outline images of large sectors of rocky coasts collected from 2012 to 2021. Observational data constitute the second section and include geomorphological, hydrogeological and biological observations collected during the swim surveys. Data are mainly collected in a series of field booklets that have been partly digitized. Geoswim is an ongoing programme, so data collection is continuing.

Observations collected during the expeditions allowed to discover many new scientific discoveries in the field of coastal geomorphology together with the discovery of new geomorphic objects, such as tidal notches in unexpected sites or unknown sea caves, mapping of coastal fauna or the precise mapping of submarine springs. These data allowed in some cases to discuss for the first time local geomorphic evolution (Furlani et al., 2017a, 2017b, 2021b), in other cases supported review studies in the Mediterranean area, such as the discussions about tidal notches (Antonioli et al., 2015, 2017), or paleogeographic studies (Lo Presti et al., 2019).

The described archive collects data useful for several purposes, such as 1) the collection of images and videos as a baseline (“0”) survey for coastal monitoring; 2) the collection of a large number of images to be

used to build 3D models of coastal landforms; 3) data for statistical analyses or 4) for geomorphological, speleological and geochemical analyses. Moreover, the archive is a valuable source of data for rocky coast management, such as creation of geosites, evaluation of risks and coastal impacts, etc., In the near future, it could integrate local cadasters, such as those of geosites or caves, or also it could be integrated in existing archives, such as those included in Giakoumi et al. (2013) or provide more data to sea level change studies.

### Declaration of competing interest

The authors declare that they have no known competing financial interests or personal relationships that could have appeared to influence the work reported in this paper.

### Data availability

Data will be made available on request.

### Acknowledgements

We are very grateful to all the friends, colleagues and students who have participated in the campaigns since 2012: more than 100 people have been involved in field surveys and project planning (see the Table in Supplementary Materials). We would also like to thank all the



MPAs (Marine Protected Areas) which have participated or supported the Geoswim project, in particular the MPA Miramare (Trieste) for field support, the MPA Isole Egadi for funding part of the fieldwork trip of Geoswim 3.0; the National Park of the Maddalena Archipelago, MPA Tavolara, and MPA Capo Caccia—Isola Piana for funding part of the fieldwork trip of Geoswim 2015 Sardinia; the Department of Geography of the University of Malta for funding part of the fieldwork trips in 2013 and 2015, MPA Isola di Ustica and MPA Isole Pelagie for field support, the Universities of Cagliari, Palermo, Trieste, Urbino, and the ENEA (*Ente Nazionale per l'Energia Alternativa*) and INGV (*Istituto Nazionale di Geofisica e Vulcanologia*) for field support. We would also like to kindly thank Egidio Trainito for the classification of organisms in the table 14.

Thanks are also owed to the Universities of Trieste and Cagliari for the use of the Punta Sardegna lighthouse.

## References

- Abadie, A., Boissery, P., Viala, C., 2018. Georeferenced underwater photogrammetry to map marine habitats and submerged artificial structures. *Photogramm. Rec.* 33 (164), 448–469.
- Akawwi, E.J., 2008. Using electrical conductivity for locating the submarine groundwater discharge along the eastern shores of the Dead Sea - Jordan. In: 11th International Multidisciplinary Scientific GeoConference SGEM2011.
- Antonoli, F., Lo Presti, V., Anzidei, M., Deiana, G., de Sabata, E., Ferranti, L., Furlani, S., Mastronuzzi, G., Orru, P.E., Pagliarulo, R., Rovere, A., Sannino, G., Sansò, P., Scicchitano, G., Spampinato, C.R., Vacchi, M., Vecchio, A., 2015. Tidal notches in Mediterranean Sea: a comprehensive analysis. *Quat. Sci. Rev.* 119, 66–84.
- Antonoli, F., Anzidei, M., Lo Presti, V., Scicchitano, G., Spampinato, C., Trainito, E., Furlani, S., 2017. Enigmatic marine notch sites: three case studies in the central Mediterranean Sea. *Quat. Int.* 439, 4–16.
- Barker, R., Dixon, L., Hooke, J., 1997. Use of terrestrial photogrammetry for monitoring and measuring bank erosion. *Earth Surf. Process. Landf.* 22 (13), 1217–1227.
- Bennett, G.L., Molnar, P., Eisenbeiss, H., McArdell, B.W., 2012. Photogrammetric analysis of slope failures feeding the head of the Illgraben debris flow channel. In: EGU General Assembly Conference Abstracts, 14, p. 10393.
- Biolchi, S., Furlani, S., Devoto, S., Gauci, R., Castaldini, D., Soldati, M., 2016a. Geomorphological identification, classification and spatial distribution of coastal landforms of Malta (Mediterranean Sea). *J. Maps* 12 (1), 87–99.
- Biolchi, S., Furlani, S., Covelli, S., Busetti, M., Cucchi, F., 2016b. Morphoneotectonics and lithology of the eastern sector of the Gulf of Trieste (NE Italy). *J. Maps* 12 (5), 936–946.
- Biolchi, S., Furlani, S., Devoto, S., Scicchitano, G., Korbar, T., Vilibić, I., Šepić, J., 2019. The origin and dynamics of coastal boulders in a semi-enclosed shallow basin: a northern Adriatic case study. *Mar. Geol.* 411, 62–77.
- Biolchi, S., Denamiel, C., Devoto, S., Korbar, T., Macovaz, V., Scicchitano, G., Vilibić, I., Furlani, S., 2020. Impact of the 29th October 2018 Vaia storm on coastal boulders in the northern Adriatic Sea. *Water* 11, 2229.
- Bisanti, L., de Sabata, E., Visconti, G., Chemello, R., 2022. Towards a local mass mortality of the Mediterranean orange coral *Astroidea calycularis* (Pallas, 1766) in the Pelagie Islands Marine protected Area (Italy). *Aquat. Conserv. Mar. Freshwat. Ecosyst.* 32 (3), 551–557.
- Busetti, A., Furlani, S., Antonoli, F., Lo Presti, V., Biolchi, S., Zavagno, E., Torricella, F., Venturini, E., Donati, S., 2015. Geoswim3.0 at Egadi Islands (Sicily, Italy): results from 70 km of swim surveying. In: Proceedings of the International Congress "Geosub - Underwater Geology", Trieste, 13-14 October 2015, pp. 27–28.
- Chandler, J., 1999. Effective application of automated digital photogrammetry for geomorphological research. *Earth Surf. Process. Landf.* 24 (1), 51–63.
- Dackombe, R.V., Gardiner, V., 1983. *Geomorphological Field Manual*. George Allen & Unwin, London.
- De Sabata, E., Vaccher, V., Guallart, J., Antonoli, F., Anzidei, M., Bellotto, M., Dal Bo, E., Furlani, S., Montagna, P., Orrù, P., Navone, A., Taviani, M., Trainito, E., Vacchi, M., 2015. Bedrock type and occurrence of *Patella ferruginea*: three case studies in north Sardinia. In: Proceedings of the International Congress Geosub 2015, Trieste, 13-14 October 2015, pp. 36–37.
- Devoto, S., Macovaz, V., Mantovani, M., Soldati, S., Furlani, S., 2020. Advantages of using UAV digital photogrammetry in the study of slow-moving coastal landslides. *Remote Sens.* 12, 3566.
- Devoto, S., Hastewell, L.J., Prampolini, M., Furlani, S., 2021. Dataset of gravity-induced landforms and sinkholes of the northeast coast of Malta (Central Mediterranean Sea). *Data* 6, 81.
- Esposito, G., Salvini, R., Matano, F., Sacchi, M., Danzi, M., Somma, R., Troise, C., 2017. Multitemporal monitoring of a coastal landslide through SfM-derived point cloud comparison. *Photogramm. Rec.* 32 (160), 459–479.
- Fawcett, D., Blanco-Sacristan, Bernaud, P., 2019. Two decades of digital photogrammetry: revisiting Chandler's 1999 paper on "Effective Application of Automated Digital Photogrammetry for Geomorphological Research" - a synthesis. *Prog. Phys. Geogr.* 43 (2), 299–312.
- Fraser, C.S., Cronk, S., 2009. A hybrid measurement approach for close-range photogrammetry. *ISPRS J. Photogramm. Remote Sens.* 64 (3), 328–333.
- Furlani, S., 2012. The Geoswim project: snorkel-surveying along 250 km of the Southern and Western Istrian Coast. *Alpine Mediterr. Quat.* 25 (2), 7–9.
- Furlani, S., 2020. Integrated observational targets and instrumental data on rock coasts through snorkel surveys. *Mar. Geol.* 425, 106191.
- Furlani, S., Biolchi, S., 2018. Le falsie costiere tra Sistiana e Villaggio del Pescatore: caratteristiche morfostrutturali e idrogeologiche. *Atti e memorie della Commissione Grotte "E. Boegan"* 47, 135–144.
- Furlani, S., Pappalardo, M., Gomez-Pujol, L., Chelli, A., 2014. The rock coast of the Mediterranean and Black Seas. In: Kennedy, D.M., Stephenson, W.J., Naylor, L.A. (Eds.), *Rock Coast Geomorphology: A Global Synthesis*. Geological Society, London Memoirs, 40, pp. 89–123.
- Furlani, S., Ninfo, A., Zavagno, E., Paganini, P., Zini, L., Biolchi, S., Antonoli, F., Coren, F., Cucchi, F., 2014b. Submerged notches in Istria and the Gulf of Trieste: results from the Geoswim Project. *Quat. Int.* 332–333, 37–47.
- Furlani, S., Antonoli, F., Cavallaro, D., Chirco, P., Caldarelli, F., Martin, F.F., Morticelli, M.G., Monaco, C., Sulli, A., Quarta, G., Biolchi, S., 2017a. Tidal notches, coastal landforms and relative sea-level changes during the Late Quaternary at Ustica Island (Tyrrhenian Sea, Italy). *Geomorphology* 299, 94–106.
- Furlani, S., Antonoli, F., Gambin, T., Gauci, R., Ninfo, A., Zavagno, E., Micallef, A., Cucchi, F., 2017b. Marine notches in the Maltese islands (central Mediterranean Sea). *Quat. Int.* 439, 158–168.
- Furlani, S., Piacentini, D., Troiani, F., Biolchi, S., Roccheggiani, M., Tamburini, A., Tricanti, E., Vaccher, V., Antonoli, F., Devoto, S., 2018. Tidal Notches (Tn) along the western Adriatic coast as markers of coastal stability during late Holocene. *Geogr. Fis. Din. Quat.* 41 (2), 33–46.
- Furlani, S., Vaccher, V., Macovaz, V., Devoto, S., 2020. A cost-effective method to create 3D models of the nearshore and intertidal zone in microtidal environments. *Remote Sens.* 12, 1880.
- Furlani, S., Kolaiti, E., Antonoli, F., Anzidei, M., Biolchi, S., Canziani, F., de Sabata, E., Iossifidis, T., Markovic, M., Marino, C., Scicchitano, G., Taviani, M., Vaccher, V., Mourtzas, N., 2021a. The Geoswim Coastal Survey of paros Island, Cyclades (Greece). In: Proceedings of the Fifth International Conference on the Archaeology of Paros and the Cyclades Paroikia, Paros, 21-24 June 2019, Athens 2021, pp. 599–610.
- Furlani, S., Vaccher, V., Antonoli, F., Agate, M., Biolchi, S., Boccali, C., Busetti, A., Caldarelli, F., Canziani, F., Chemello, R., Deguara, J.C., Dal Bo, E., Dean, S., Deiana, G., De Sabata, E., Donno, Y., Gauci, R., Giaccione, T., Lo Presti, V., Montagna, P., Navone, A., Orrù, P.E., Porqueddu, A., Schembri, J.A., Taviani, M., Torricella, F., Trainito, E., Vacchi, M., Venturini, E., 2021b. Preservation of MIS 5.5 erosional landforms and biological structures to be used as sea level change markers: a matter of luck. *Water* 13 (15), 2127.
- Gaglianone, G., Crognale, J., Esposito, C., 2018. Investigating submerged morphologies by means of the low-budget "GeoDive" method (high resolution for detailed 3D reconstruction and related measurements). *ACTA IMEKO* 7 (2), 50–59.
- Giakoumi, S., Sini, M., Gerovasileiou, V., Mazar, T., Beher, J., Possingham, H.P., Abdulla, A., Cinar, M.E., Dendrinou, P., Gucu, A.C., Karamanlidis, A.A., Rodic, P., Panayotidis, P., Taskin, E., Jaklin, A., Voultsiadou, E., Webster, C., Zenetos, A., Katsanevakis, S., 2013. Ecoregion-based conservation planning in the Mediterranean: dealing with large-scale heterogeneity. *PLoS ONE* 8 (10), e76449.
- Goudie, A., 1990. *Geomorphological Techniques*, Second edition. Routledge, London and New York.
- Jou-Claus, S., Folch, A., Garcia-Orellana, J., 2021. Applicability of Landsat 8 thermal infrared sensor for identifying submarine groundwater discharge springs in the Mediterranean Sea basin. *Hydro Earth Syst. Sci.* 25, 4789–4805.
- Kennedy, D.M., Stephenson, W.J., Naylor, L.A., 2014. Introduction to the rock coasts of the world. *Geol. Soc. Lond. Mem.* 40 (1), 1–5.
- Levin, L.A., Bett, B.J., Gates, A.R., Heimbach, P., Howe, B.M., Janssen, F., McCurdy, A., Ruhl, H.A., Snelgrove, P., Stocks, K.L., Bailey, D., Baumann-Pickering, S., Beaverson, C., Benfield, M.C., Booth, D.J., Carreiro-Silva, M., Colaço, A., Eblé, M.C., Fowler, A.M., Gjerde, K.M., Jones, D.O.B., Katsumata, K., Kelley, D., Le Bris, N., Leonardi, A.P., Lejzerowicz, F., Macreadie, P.I., McLean, D., Meitz, F., Morato, T., Netburn, A., Pawlowski, J., Smith, C.R., Sun, S., Uchida, H., Vardaro, M.F., Venkatesan, R., Weller, R.A., 2019. Global observing needs in the deep ocean. *Front. Mar. Sci.* 6, 241.
- Lo Presti, V., Antonoli, F., Palombo, M.R., Agnesi, V., Biolchi, S., Calcagnile, L., Di Patti, C., Donati, S., Furlani, S., Merizzi, J., Pepe, F., Quarta, G., Renda, P., Sulli, A., Tusa, S., 2019. Palaeogeographical evolution of the Egadi Islands (western Sicily, Italy): implications for late Pleistocene and early Holocene Sea crossing by humans and other mammals in Western Mediterranean. *Earth Sci. Rev.* 194, 160–181.
- Mattei, G., Troisi, S., Aucelli, P.P.C., Pappone, G., Peluso, G., Stefanile, M., 2019. Multiscale reconstruction of natural and archaeological underwater landscape by optical and acoustic sensors. In: 2018 IEEE International Workshop on Metrology for the Sea: Learning to Measure Sea Health Parameters, MetroSea 2018 – Proceedings, 8657872, pp. 46–49.
- Micheletti, N., Foresti, L., Robert, S., Leuenberger, M., Pedrazzini, A., Jaboyedoff, M., Kanevski, M., 2014. Machine learning feature selection methods for landslide susceptibility mapping. *Math. Geosci.* 46 (1), 33–57.
- Miragoli, M., 1994. Le grotte delle Egadi, contributo aggiuntivo. *Boll. Accad. Gioenia Sci. Nat.* 27 (348), 413–434.

- Moore, P.J., Martin, J.B., Sreaton, E.J., 2009. Geochemical and statistical evidence of recharge, mixing, and controls on spring discharge in an eogenetic karst aquifer. *J. Hydrol.* 376, 443–455.
- Morucci, S., Picone, M., Nardone, G., Arena, G., 2016. Tides and waves in the Central Mediterranean Sea. *J. Oper. Oceanogr.* 9 (1), s10–s17.
- Pitman, S.J., 2014. 3.2.6. Methods for field measurements and remote sensing of the swas zone. In: British Society for Geomorphology. *Geomorphological Techniques*, pp. 1–14. Chap. 3, Sec. 2.6.
- Stieglitz, T., Rapaglia, J., Bokuniewicz, H., 2008. Estimation of submarine groundwater discharge from bulk ground electrical conductivity measurements. *J. Geophys. Res.* 113, C08007.
- Sunamura, T., 1992. *Geomorphology of Rocky Coasts*. John Wiley & Sons, Chichester.
- Swirad, Z.M., Rosser, N.J., Brain, M.J., 2019. Identifying mechanisms of shore platform erosion using Structure-from-Motion (SfM) photogrammetry. *Earth Surf. Process. Landf.* 44 (8), 1542–1558.
- Trenhaile, A.S., 1987. *The Geomorphology of Rock Coasts*. Oxford University Press, USA.
- Wynn, R.B., Huvenne, V.A., Le Bas, T.P., Murton, B.J., Connelly, D.P., Bett, B.J., Ruhl, H. A., Morris, K.J., Peakall, J., Parsons, D.R., Sumner, E.J., Darby, S.E., Dorrell, R.M., Hunta, J.E., 2014. Autonomous Underwater Vehicles (AUVs): their past, present and future contributions to the advancement of marine geoscience. *Mar. Geol.* 352, 451–468.
- Yoerger, D.R., Jakuba, M., Bradley, A.M., 2007. Techniques for deep sea near-bottom survey using an autonomous underwater vehicle. *Int. J. Robot.* 26 (1), 41–54.